Atmospheric Environment 187 (2018) 9–23

Contents lists available at ScienceDirect

Atmospheric Environment

journal homepage: www.elsevier.com/locate/atmosenv

Monitoring of greenhouse gases and pollutants across an urban area using a light-rail public transit platform

Logan E. Mitchell[a,*], Erik T. Crosman[a], Alexander A. Jacques[a], Benjamin Fasoli[a], Luke Leclair-Marzolf[a], John Horel[a], David R. Bowling[b], James R. Ehleringer[b], John C. Lin[a]

[a] Department of Atmospheric Sciences, University of Utah, Salt Lake City, UT, United States
[b] Department of Biology, University of Utah, Salt Lake City, UT, United States

GRAPHICAL ABSTRACT

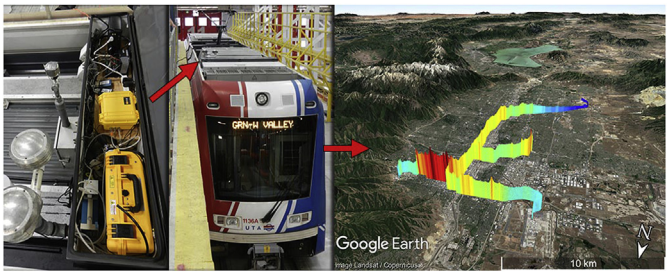

ARTICLE INFO

Keywords:
Urban atmosphere
Greenhouse gas
Air pollution
Spatial pattern
Temporal pattern
Mobile monitoring

ABSTRACT

Anthropogenic emissions within urban environments are characterized by spatial heterogeneity and temporal variability that present challenges for measuring urban greenhouse gases and air pollutants. To address these challenges, we mounted instruments on public transit light-rail train cars that traverse the metropolitan Salt Lake Valley (SLV) in Utah, USA to observe the temporal and spatial variability of atmospheric species including carbon dioxide (CO_2), methane (CH_4), ozone (O_3), fine particulate matter ($PM_{2.5}$), and nitrogen dioxide (NO_2). Utilizing electrified light-rail public transit as an observational platform enables real-time measurements with low operating costs while avoiding self-contamination from vehicle exhaust. We examine temporal averages and case studies of each species that reveal gradients, intermittent point sources, seasonal and diel changes, and complex relationships resulting from emissions, atmospheric chemistry, and meteorological conditions. CO_2 and NO_2 are related through the combustion of fossil fuel and we observed a broad spatial gradient across the city as well distinct plumes at traffic intersections and, for NO_2, a large plume adjacent to a locomotive rail yard. Distributions of O_3 were strongly correlated with NO_2 due to atmospheric photochemical and titration processes. Episodes of high $PM_{2.5}$ had distinct spatial patterns depending on meteorological conditions during wintertime persistent cold-air pool episodes. The spatial pattern of CH_4 was characterized by distinct plumes associated with industrial and commercial facilities, some of which followed temporal patterns indicative of daytime working hours; other plumes were persistent throughout the whole day, suggestive of leak-related fugitive emissions. The ongoing multi-year record of spatial and temporal air quality observations provides a valuable data set for future air quality exposure studies. Our results suggest pollution and greenhouse gas emission monitoring and exposure assessment could be greatly enhanced by deploying instruments on public transit systems in urban centers worldwide.

* Corresponding author.
E-mail address: logan.mitchell@utah.edu (L.E. Mitchell).

https://doi.org/10.1016/j.atmosenv.2018.05.044
Received 23 December 2017; Received in revised form 21 May 2018; Accepted 23 May 2018
Available online 25 May 2018
1352-2310/

1. Introduction

Trace species in the atmosphere have a wide range of impacts including climate change, health, and ecosystem impacts. Metropolitan areas are characterized by concentrated emissions and large intra-urban spatiotemporal variability of greenhouse gases (GHGs) and pollutants (Baldauf et al., 2008; Christen et al., 2011). Poor urban air quality leads to impacts on human health (e.g. respiratory, circulatory, cancer, mortality, etc. (Di et al., 2017; Landrigan et al., 2017)) as well as cascading economic impacts (e.g. health care costs, decreased worker productivity, etc. (Zivin and Neidell, 2018)) and environmental impacts (e.g. O_3 injury to plants, viewshed impacts from haze, etc. (U.S. EPA, 2013)). Detailed observations and models are needed to resolve the intra-urban environment in order to link human health impacts to pollutant variability and to investigate the anthropogenic, chemical, and meteorological factors controlling the variability in urban GHGs and pollutants as cities are growing (Gurney et al., 2015; Park and Kwan, 2017; Venkatram et al., 2009). While models of emissions have improved in temporal and spatial resolution (e.g. (Gurney et al., 2009; Hoek et al., 2008; Pouliot et al., 2012) the ability of current urban monitoring networks to provide constraints for these models remains limited (Air Quality Research Subcommittee, 2013; Hutyra et al., 2014).

Currently, numerous observational configurations exist to monitor ambient concentrations of trace species across urban areas for research or regulatory purposes. Examples include monitors for U.S. Environmental Protection Agency (US EPA) Criteria Air Pollutants to comply with the regulatory requirements of the Clean Air Act, or the National Oceanic and Atmospheric Administration's Global Greenhouse Gas Reference Network that is used to conduct research on the global carbon cycle. These observations, located at fixed sites, have been maintained for decades with high precision and accuracy, and have resulted in numerous insights into health consequences of pollutants (Correia et al., 2013) or the impacts of trace species on global climate (Le Quéré et al., 2016). However, sparse networks of stationary sites are intended to monitor air quality across large spatial scales (regional or counties) and cannot resolve spatial heterogeneities that are known to exist within urban environments.

As atmospheric monitoring instrumentation decreases in size and cost, the paradigm for urban air monitoring has evolved to include higher spatial resolution (Kumar et al., 2015; Snyder et al., 2013). It has become possible to deploy dense networks of temporary or permanent fixed sites that can resolve intra-urban spatial patterns (e.g., (Deville Cavellin et al., 2016; Jiao et al., 2016; Matte et al., 2013; Shusterman et al., 2016). These dense networks typically consist of many instruments that present maintenance and calibration challenges over time (Borrego et al., 2016; Kelly et al., 2017; Miskell et al., 2016; Thompson, 2016). In the last several years, a proliferation of low-cost sensors driven by citizen science initiatives and the rapid development of micro-sensor technology has dramatically increased air quality data collection across urban landscapes, but more research on how to calibrate these low-cost sensors with research-grade instrumentation is needed (Barakeh et al., 2017; Clements et al., 2017; Zimmerman et al., 2017). Assessing intra-urban spatial patterns has also been undertaken for research applications by deploying sensors on mobile platforms (Gozzi et al., 2016) such as automobiles, aircraft, and bicycles (e.g., (Apte et al., 2017; Hopkins et al., 2016; Lee et al., 2017; Mays et al., 2009; Van den Bossche et al., 2015). While mobile platforms improve spatial coverage, labor costs are often considerable, limiting the long-term deployability of such mobile platforms. Hence, it is difficult to conduct manned mobile monitoring campaigns to assess changes over time or to characterize the impact of intermittent emissions on ambient concentrations without considerable cost. While both mobile and stationary sampling approaches have benefits and challenges, a well-defined best practice for sustained monitoring at fine scales of urban atmospheric trace species has remained elusive.

Here we present a new project that facilitates routine real-time monitoring of intra-urban atmospheric trace species using research grade instruments mounted on public transit light-rail vehicles that transect the Salt Lake Valley (SLV) metropolitan area at routine intervals. To our knowledge, only a few mobile urban observation networks leveraging public transit currently exist worldwide: Zurich, Switzerland (Hasenfratz et al., 2015); Karlsruhe, Germany (Hagemann et al., 2014); Oslo, Norway (Castell et al., 2015); and Perugia, Italy (Castellini et al., 2014). Each of these projects have different experimental designs with a different suite of measurements, and while their utility is still being explored, it has been shown that public transit based monitoring can be used to create high-resolution maps of air pollution across urban areas (Hasenfratz et al., 2015). Our study is the first effort to utilize public transit for urban observations of trace species in North America. Starting in December 2014, we partnered with the Utah Transit Authority (UTA) and installed instrumentation to measure carbon dioxide (CO_2), methane (CH_4), ozone (O_3), and fine particulate matter ($PM_{2.5}$) in a secure box on the roof of an electrically-powered light-rail public transit train (aka “TRAX”). A second suite of sensors on another TRAX train car was added in February 2016. Basic meteorological parameters (temperature, relative humidity, and pressure) were also measured. Additionally, temporary installations of instruments that measure black carbon and nitrogen dioxide (NO_2) were deployed for short periods. To facilitate public engagement, real-time data were transmitted to University of Utah servers every 5 min and made accessible via web-based visualizations (http://air.utah.edu/ and http://meso1.chpc.utah.edu/mesotrax/).

The SLV, with a population of just over 1 million people, experiences on average 40 days annually of pollutant levels (including both summer and winter pollutant episodes) exceeding the U.S. National Ambient Air Quality Standards (NAAQS) resulting from a combination of meteorological patterns, topography, and emissions. In the winter, elevated levels of $PM_{2.5}$ result from emissions accumulating in persistent cold air pools (PCAPs; locally known as temperature inversions). On average, 6.8 PCAPs occurred each winter, with an average duration of 3.1 days, that exceeded the NAAQS for $PM_{2.5}$ of 35 $\mu g\, m^{-3}$ on average 18 days per winter, however with considerable interannual variability (Whiteman et al., 2014). During winter, the maximum (minimum) temperatures were 3.5 (−6) °C and average snowfall was 110 cm. The snow cover reflected incoming radiation, maintaining cool surface temperatures and enhanced nocturnal surface radiative cooling, resulting in stronger wintertime PCAPs when snow cover was present. During summer the average maximum (minimum) temperatures were 32 (16) °C, but there were frequent high-pressure ridges over the Western US that resulted in prolonged periods of elevated heat and stagnation. These meteorological conditions, in combination with urban precursor emissions and wildfire smoke, led to the photochemical production of elevated ground level O_3 that exceeded the NAAQS for O_3 of 70 ppb on average 22 days per year (Horel et al., 2016). Public awareness of the health risks associated with summertime O_3 is less than for wintertime $PM_{2.5}$ because O_3 is invisible, and high concentrations are often accompanied by fair weather. Episodic air quality reductions also result from dust storms and wild fires several times each year (Mallia et al., 2017, 2015; Steenburgh et al., 2012). As a result of all of these factors, intense public interest in improving air quality exists, as demonstrated by the 2016 Utah Foundation survey of voter's concerns that found air quality among the public's most pressing issues (Bateman et al., 2016). Finally, because of the number of NAAQS exceedances, The Utah Division of Air Quality (DAQ) is currently engaged in developing a State Implementation Plan (SIP) to improve air quality to bring the state into compliance with the Clean Air Act.

In addition to air quality concerns, Salt Lake City has adopted aggressive greenhouse gas emission reduction targets (Salt Lake City Corporation, 2016) that, if successful, will result in observable reductions in concentrations of GHGs in the city in the coming years. Many other public and private stakeholders are also engaged in GHG

mitigation efforts as well.

Several complimentary resources are available that could assist in evaluating and utilizing the TRAX based observations. These include a high-density meteorological observation network (Horel et al., 2016), a GHG monitoring network (Mitchell et al., 2018), a growing low-cost citizen-science led network of air quality monitors (Kelly et al., 2017) (https://www.purpleair.com/), a small network of research-grade fixed air quality monitoring stations (Baasandorj et al., 2017), and detailed emissions models (Patarasuk et al., 2016). The combination of poor air quality, wide ranging interest from the public, stakeholders, governments and regulators, as well as several complimentary resources make the SLV a unique testbed for evaluating a public transit based atmospheric observation system (Lin et al., in press).

In this paper our main goal is to provide an overview of an ongoing light-rail public transit-based observation project that has measured air pollutants and GHGs across an urban area at high resolution for the past 3 years. We describe our experimental design, present examples of how these observations can be utilized, and discuss future directions for mobile observations deployed on public transit platforms.

2. Materials and methods

2.1. TRAX light rail network

The SLV contains the state capital, Salt Lake City, and is located within Salt Lake County, Utah in the inter-mountain west of the continental U.S. (Fig. 1). It is bounded by the Wasatch and Oquirrh Mountains on the east and west sides of the valley, the Traverse Mountains to the south, and the Great Salt Lake to the northwest. The TRAX light rail train network consists of over 145 electric trains servicing three lines (Red, Green, and Blue) along 94 km of rail track that provide coverage across the SLV (Fig. 1). Urbanization along the rail lines varies from dense urban downtown regions to suburban and rural settings, and the train travels on and off major roadways. TRAX operates an older model of rail car on the Blue line, so our data are almost exclusively from the Red and Green lines. Along the Red and Green lines there are 25 and 18 passenger stops, and it takes 60 and 46 min, respectively, to complete a transect on each line. In addition to the spatial coverage, the Red line also provides a 225 m pseudo-vertical profile from the valley floor (1285 m) to the surrounding mountain foothills (1510 m). Each TRAX train car covers 18–24 transects when operating for a full day (approximately 18 h from 5 a.m. to midnight). During the period December 2014–April 2017, the trains have been deployed 760 days comprising 10,300 transects (averaging 14 transects a day and deployed 61% of days, or ~4 days a week). When the trains were not in operation, they were often parked outside and therefore became periodic stationary observation sites that provided additional observations. Several complementary stationary GHG and air pollutant stations were located in close proximity to the TRAX route that can be used to evaluate the TRAX based measurements. This includes the DAQ Hawthorne site as well as several University of Utah air quality and GHG monitoring sites (Fig. 1).

2.2. Instrumentation set-up

Two TRAX trains (numbered 1 136 and 1104, hereafter TRAX 1 and 2) were outfitted with sensors to measure air quality, GHGs, and meteorological parameters. Electrified trains are an ideal platform for air sampling because they have zero direct emissions and often run continuously throughout the day. The trains have electric circuitry on their roofs in steel weatherproof boxes, and our instruments were installed in one of the spare boxes (dimensions 1.5 m × 0.5 m x 0.5 m). The sample inlets extended 0.5 m above the top of the train through a pipe protruding from the metal box topped with a vent cover and were 4 m above ground level. AC power was provided with a connection into the cabin accessory outlets. Two generic computer fans provided cooling

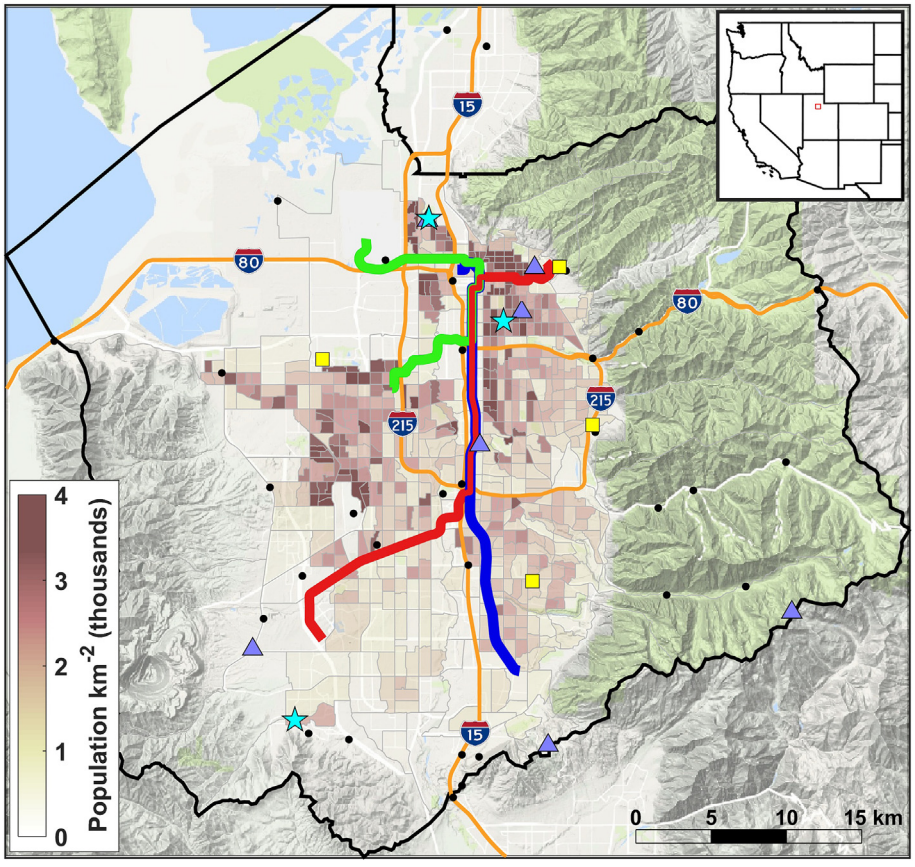

Fig. 1. The TRAX Red, Green, and Blue train lines in the Salt Lake Valley (SLV). The University of Utah greenhouse gas monitoring network (blue triangles), research grade air quality stations (yellow squares), surface weather stations courtesy of MesoWest (black dots (Horel et al., 2002)), and the Utah Division of Air Quality's Hawthorne site (cyan star 2 km east of where the Green and Red lines overlap) are also shown. The population density is superimposed in brown shading, and the inset shows the location of the SLV as a red box in the western U.S. (For interpretation of the references to colour in this figure legend, the reader is referred to the Web version of this article.)

Table 1
Measurement equipment deployed on TRAX train cars.

Instrument	Species	Sample rate	Measurement uncertainty	TRAX Train car
Met One Instruments E-Sampler	$PM_{2.5}$	1 min.	1 μg m^{-3}	1
Met One Instruments ES-642 Remote Dust Monitor	$PM_{2.5}$	1 s.	1 μg m^{-3}	2
2 B Technologies Model 205 Ozone Monitor	O_3	2 s.	2%	1 and 2
Los Gatos Research Ultra-portable Greenhouse Gas Analyzer	CO_2 CH_4 H_2O	1 s.	0.3 ppm CO_2 2 ppb CH_4 100 ppm H_2O	1
Los Gatos Research NO_2 Analyzer	NO_2	1 s.	0.05 ppb	2

for the instruments in the box in the summer. Table 1 lists the equipment installed on the TRAX trains, their sampling frequency, and their measurement accuracy as reported by the equipment manufacturers. The Campbell Scientific CS215-L Temperature and Relative Humidity probe and CS106 Barometer were used for the meteorological parameters. Data were recorded by a Raspberry Pi based data logger (which also controlled a valve systems for hourly automated GHG calibrations) and a Campbell Scientific data logger (CR1000). The observations were transmitted to University of Utah servers via cellular communications every 5 min. Fig. 2 summarizes the temporal data coverage by species between the start of the project through April 2017. Gaps in the data resulted from a variety of factors including train maintenance, instrument maintenance, and periods when instrument calibration parameters were unknown or unavailable (Fig. 2). A greater number of train transects per month occurred when we requested enhanced observations during intensive field campaigns (e.g., summer 2015 and winter 2017), while decreased numbers of train transects per month occurred when the trains were undergoing maintenance.

To examine the mean variability in GHG and air pollutants over various time periods (e.g., average summertime O_3, or annual GHGs), we calculated averages along the rail track using available transects during these periods. This was carried out by creating a track of approximately equally spaced (~35–40 m) points along each of the train lines. Then for each transect of the train from one end of a line to the other, the data were assigned to the nearest equally spaced point along the track. Since the spacing of the points is suited for a 1-Hz sampling frequency, we linearly interpolated the observations from the E-Sampler and 2 B Ozone monitors to a 1-Hz sampling rate. If there were multiple observations at a single point (e.g. during a 45 s stop at a station where passengers boarded the train), the observations were averaged, resulting in equal spatial extent for data along each train transect. These transects could then be averaged over selected temporal periods to create a spatially explicit, temporally averaged composite of the data.

In order to correctly interpret the spatial observations, the GPS location data must be precisely synchronized with the atmospheric measurements. A time lag between the GPS and other measurements can arise from a misalignment in the clocks, but this was addressed by recording a common time stamp from the data logger to all of the data files. A secondary time lag can result from the amount of time it takes for a parcel of air to travel the length of the inlet tubing to the instrument. This was addressed empirically by identifying stationary features in the data (point source emissions, freeway, etc.) and specifying a time lag such that the feature occurs in the same place when the train was traveling in both directions (Fig. 3). This led to a higher correlation between data averaged when the train was traveling in both directions. Time lags varied between instruments and with changes in tubing but were in the range of 1–15 s.

Calibration of the GHG measurements was conducted hourly using a working reference gas tank with known near ambient CO_2 and CH_4 mole fractions tertiary to the World Meteorological Organization X2007 CO_2 mole fraction scale (Zhao and Tans, 2006) and the NOAA04 CH_4 mole fraction scale (Dlugokencky et al., 2005). The ozone monitors, which have been approved by US EPA as a Federal Equivalent Method (FEM), were calibrated from either the manufacturer or at a DAQ facility, while the $PM_{2.5}$ sensors were calibrated by the manufacturer approximately annually. The NO_2 analyzer has an internal metal oxide scrubber that produces NO_2-free air that provides a zero calibration every 30 min that were subtracted from the observations. Since this instrument was installed temporarily, the NO_2 span was only calibrated twice during the year-long deployment with two different sets of

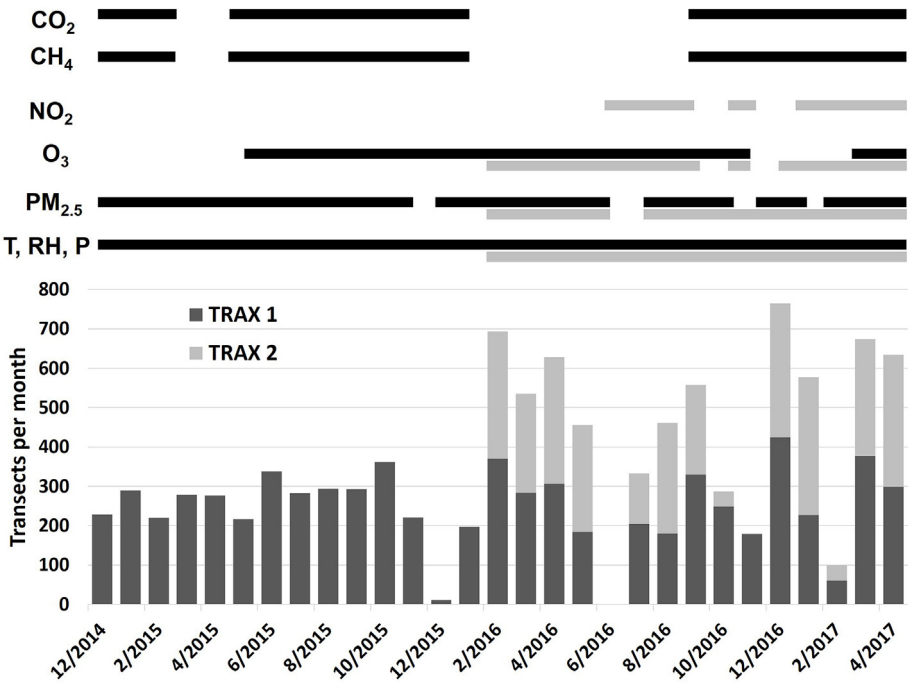

Fig. 2. Temporal data coverage by species measured (top) and by transect count (bottom).

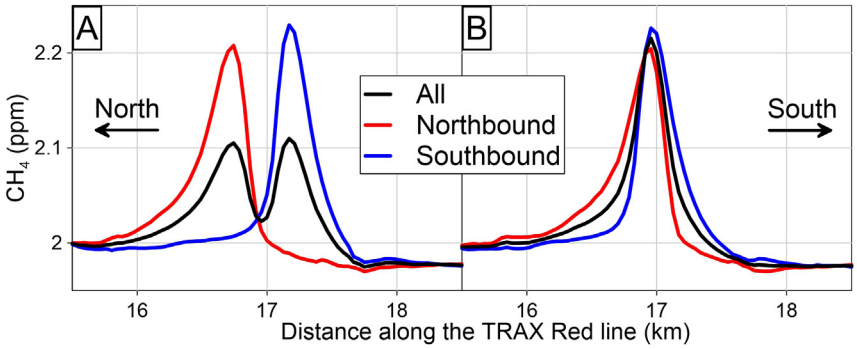

Fig. 3. Example of an empirical determination of the time lag due to the amount of time it takes for a parcel of air to travel the length of the inlet tubing to the instrument. In the raw data, without a lag time applied to the data, a persistent feature in the CH_4 measurements along the Red TRAX line was shifted north (south) of the central location when the train was traveling northbound (southbound) (A). When a time lag was applied to the data (in this case a 9-s lag) the peak occurred in the same location when the northbound and southbound data were averaged (B). (For interpretation of the references to colour in this figure legend, the reader is referred to the Web version of this article.)

calibration equipment. In both cased there was an excellent linear response ($R^2 > 0.99$) but the slope of the line at the start of the deployment was 1.07 and at the end it was 0.88. We did not correct for this change over time because of the infrequency of the span calibrations and because of the different calibration equipment used. Thus, while there is likely a ± 10% uncertainty in the absolute magnitude of the NO_2 observations, prior work has found that the span changes slowly over time (Brent et al., 2013), so the relative magnitude of the spatial patterns across the city are robust.

2.3. Evaluation against stationary sites

To evaluate our mobile measurements, we compared the TRAX observations to observations made at two stationary measurement sites located near the TRAX train lines (Fig. 4). We evaluated the TRAX observations against the Utah Division of Air Quality (DAQ) Hawthorne site maintained by the state of Utah for US EPA regulatory purposes that is 2 km east of the train line along a section where the Red and Green lines overlap, as well as the University of Utah (UOU) site located 0.6 km north of the TRAX Red line in the northeast part of the SLV (Fig. 1). The goal was to provide representative comparisons and an overall sense of the robustness of the TRAX data. Future work should include more detailed comparisons and include fixed sites co-located next to the TRAX train line, depending on species of interest.

For $PM_{2.5}$ we compared the TRAX observations against the hourly DAQ measurements that utilized a FEM for the month of February 2016. This time period was chosen because there was a persistent cold air pool (PCAP) event and PCAP events tend to have a large dynamic

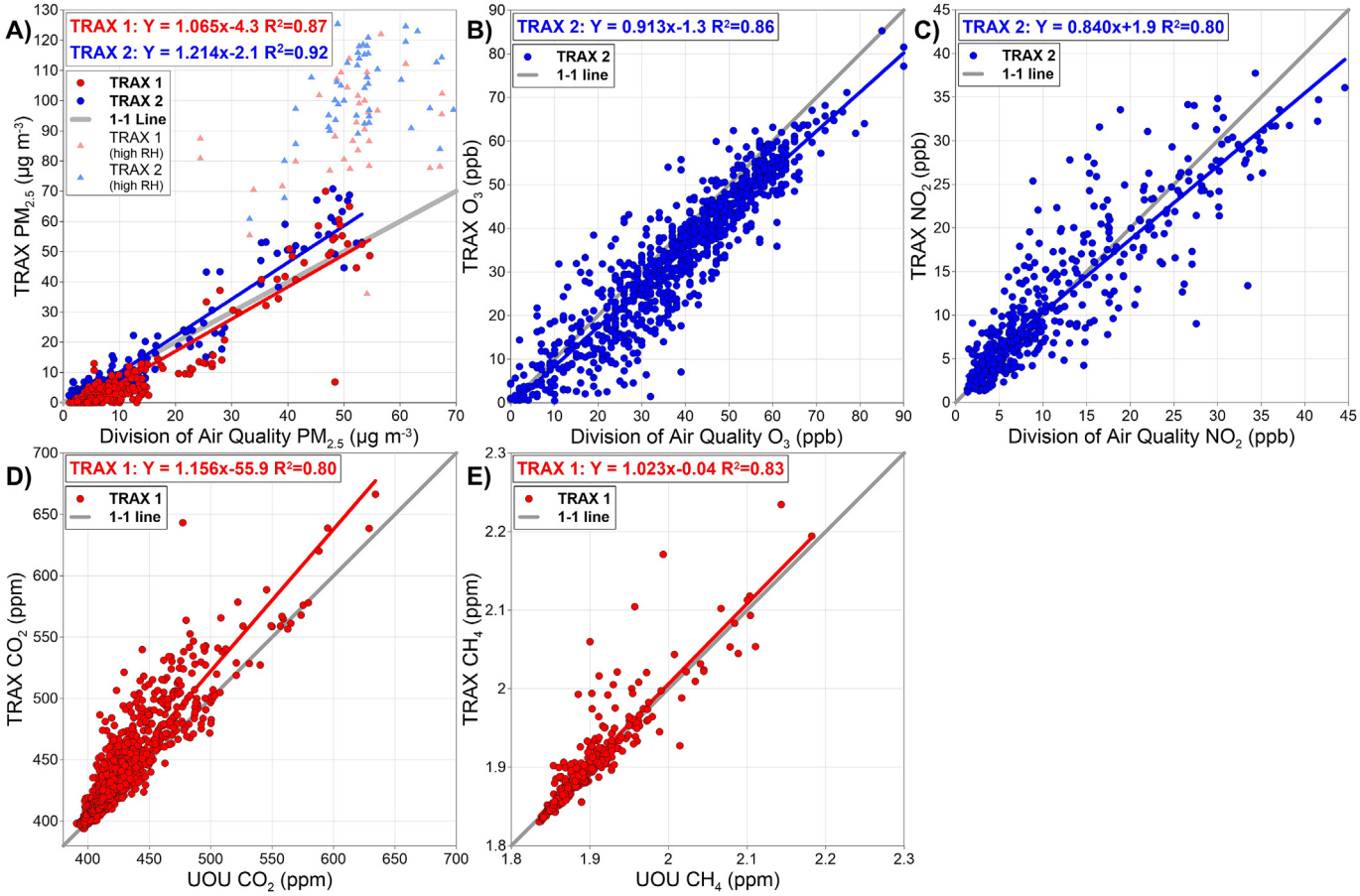

Fig. 4. Comparisons of TRAX measurements against measurements made at stationary sites. The top row (panels A–C) shows comparisons of air pollutants $PM_{2.5}$, O_3, and NO_2 against the Utah Division of Air Quality Hawthorne site (cyan star in Fig. 1) while the bottom row (panels D and E) shows comparisons of greenhouse gases CO_2 and CH_4 against the UOU site (the northeastern most blue triangle adjacent to the Red line in Fig. 1). (For interpretation of the references to colour in this figure legend, the reader is referred to the Web version of this article.)

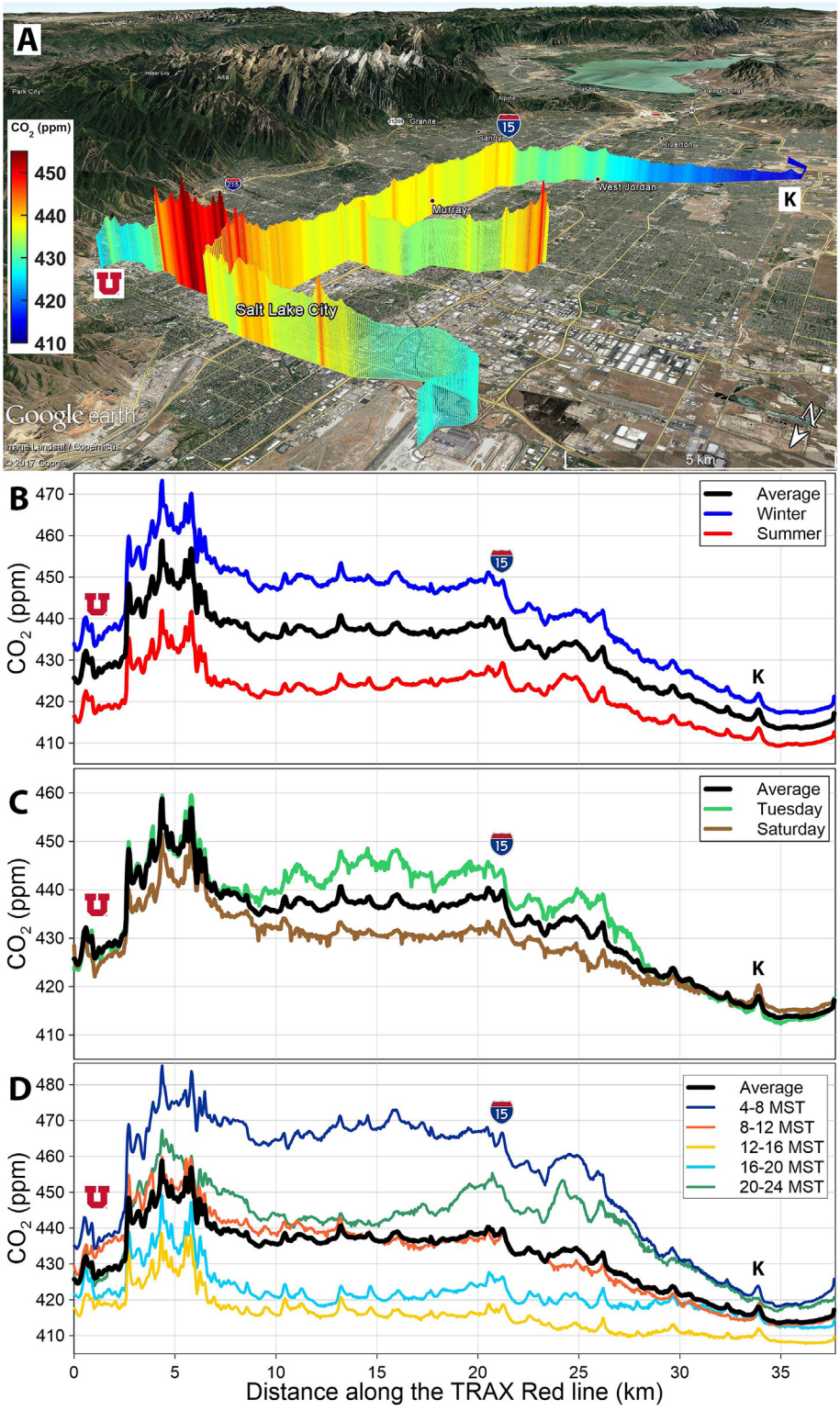

Fig. 5. Spatially and temporally averaged carbon dioxide (CO_2) in the SLV between December 2014 and April 2017 along the Red and Green TRAX train lines (A). The lower panels show seasonal (B), day of week (C), and diel (D) averages, as compared to the overall average that is shown in panel A (the overall average is indicated by the black line in panels B–D). Winter (summer) months were averaged over October–March (April–August). The location of the University of Utah and the UOU stationary measurement site on the northeastern foothills of the SLV is indicated with a red 'U'. Also, the location where the Red line crosses the I-15 interstate freeway, and where it passes next to a brick factory are indicated with an I-15 placard and a 'K', respectively. (For interpretation of the references to colour in this figure legend, the reader is referred to the Web version of this article.)

range in $PM_{2.5}$ and often do not have fine scale spatial variability (Baasandorj et al., 2017), as discussed in the $PM_{2.5}$ results section below. Thus, for this time period, the TRAX measurements should be comparable to those at the DAQ monitoring station 2 km east of the train line. The TRAX observations were averaged over a 2.3 km long section of the train line as well as subsections where the train was moving and where it was stopped at two train stops. While the temporal spans of the measurements were different (a few minutes on TRAX vs. Hourly average at DAQ), this was the most accessible comparison to evaluate the TRAX measurements against a FEM monitoring station. We observed a good correlation for most of the month (circles); however, in the middle of the PCAP event the ambient relative humidity (RH) increased and caused the TRAX instruments to record anomalously high $PM_{2.5}$ concentrations (triangles), due to hygroscopic swelling of particles, causing the nephelometer to overestimate the $PM_{2.5}$ concentration. The MetOne $PM_{2.5}$ analyzers on the two trains both use onboard heaters to dry the air prior to measurement and we have found that they are unable to suitably dry the air when ambient relative humidity is greater

than ~85%. These high relative humidity conditions were infrequent and are easily identified by comparisons with the DAQ monitor, so they did not pose a problem for our experimental design and we have removed these periods from the data set. The good agreement with high R^2 values during normal operations exist regardless of whether the train was in motion or stationary, indicating that our experimental setup was not sensitive to the speed of the train (not shown).

For O_3 and NO_2 we also compared the TRAX measurements to the hourly DAQ measurements. We examined these relationships for the entire year NO_2 measurements were available (June 2016–June 2017) but found that the slope of the relationships changed during the winter, when oxidant titration could at times lead to complete titration of O_3 (Baasandorj et al., 2017). Therefore, we excluded the winter months (November–February) from the comparison. For this comparison we again found high correlations ($R^2 \geq 0.8$) that give confidence in the TRAX-based mobile observations.

For the GHGs we compared the TRAX measurements and those at the UOU site during a time period with good data coverage from June-October, 2015. We averaged the TRAX observations over a 1-km section of the track and compared them to the UOU observations over the same time period (~50 s duration). Both CO_2 and CH_4 measurements had high correlations ($R^2 > 0.8$), indicating good overall agreement. The scatter in the comparisons is likely due to the proximity of local sources (traffic and fugitive CH_4 emissions).

3. Results and discussion

In the following sections, we provide examples of the observed variations in GHGs and criteria pollutants observed with the TRAX platform. Human and natural factors such as emissions from on-road, industrial and residential sources, as well as chemical processes, meteorology, and topography affect the observed concentrations. The complex wind flow patterns and vertical stability owing to the unique meteorology and topography of the SLV control to a large degree the transport and mixing of trace species in the boundary-layer. The daily cycle of heating and cooling in a mountain valley combined with thermal contrasts between the Great Salt Lake and the SLV results, in the absence of strong winds associated with synoptic weather systems, in down-valley flow (from south to north) at night and up-valley flow (from north to south) during the day throughout the year (Blaylock et al., 2016; Crosman and Horel, 2016; Horel et al., 2016). These thermally-driven circulation patterns combine with terrain-flow interactions (Lareau and Horel, 2015, 2014) and variations in boundary-layer depth (Whiteman et al., 2014; Young and Whiteman, 2015) to impact pollutant variability across the SLV. In addition, emissions and chemical reactions (e.g., point sources and the distance to roadway) within the complex urban landscape also drive patterns in trace species (Horel et al., 2016). All of the data shown in the figures and the native Google Earth KMZ files are included in the Supplementary Materials.

3.1. Greenhouse gases

3.1.1. Carbon dioxide (CO_2)

The average CO_2 mole fractions in the SLV from available transects during the duration of the project (December 2014–April 2017) shows spatial patterns across roadway, neighborhood, and urban scales (Fig. 5a). Across the metropolitan region, CO_2 mole fractions were higher in the urban center and along the north-south urban corridor in the center of the SLV while lower mole fractions were visible along the urban periphery and were lowest in the southwestern SLV near the edge of the suburban margin of the urbanized area. This mole fraction gradient pattern (sometimes referred to as an 'urban dome' (Idso et al., 2001); however this terminology can be misinterpreted because the measurements are all at the surface and do not characterize vertical distributions) was created by the density of emissions from the on-road, residential, commercial, and industrial sectors across the urban landscape. The SLV has one of the longest running multi-site urban CO_2 monitoring networks in the world, consisting of five sites that began operation in 2001 (Mitchell et al., 2018), which can be compared to the TRAX spatiotemporal averages. While the broad structure of the urban gradient across the SLV is observable at the fixed sites, the TRAX observations resolve the spatial structure of mole fraction gradients across the metropolitan region in much finer detail than is possible from a small number of fixed sites.

In addition to the broad spatial pattern across the city, there were smaller-scale features that were visible in the averages. Elevated CO_2 mole fractions were found along every road that the train crosses. On the Red line between the urban center and the University of Utah (2.5–6.5 km along the Red line in Fig. 5), the rail tracks were located in the middle of a four-lane road with heavy automobile traffic (> 20,000 vehicles day^{-1} in 2014 (UDOT, 2017)) and surrounded by multi-story buildings that act as an urban canyon and could reduce ground level atmospheric mixing. This combination of factors resulted in the highest CO_2 mole fractions we observed along the TRAX lines. In other areas, the train ran on a dedicated transit corridor that was not adjacent to tailpipe emissions, was in the vicinity of roads with less traffic, or was surrounded by shorter buildings, and these factors resulted in lower CO_2 mole fractions.

One advantage of using a transit-based observation platform is its ability to make repeated transects on a regular basis that provides unprecedented temporal coverage for a mobile platform. With this data we can examine the spatial pattern of CO_2 mole fractions during different seasons (Fig. 5b), days of the week (Fig. 5c), and hours of the day (Fig. 5d). These comparisons reveal higher mole fractions at night and during the winter months due to lower planetary boundary layers during these time periods and, during the winter, greater emissions from combustion of natural gas for home heating (Mitchell et al., 2018; Pataki et al., 2003). Lower mole fractions during the day were caused by greater atmospheric mixing as well as photosynthetic uptake of CO_2 from vegetation. The magnitude of the seasonal and diel cycles were much larger along the urban corridor where there were greater anthropogenic emissions than there were at the southwestern end of the Salt Lake Valley at the margin of the urbanized area (~35 km in Fig. 5b). The mole fractions along the urban corridor (10–27 km in Fig. 5c) were also higher during the week than during the weekend due to greater levels of traffic, but this difference was not as large in the downtown core of the city (5–7.5 km in Fig. 5c). These examples illustrate the rich temporal coverage that is possible with a public-transit based measurement platform.

3.1.2. Methane (CH_4)

Numerous studies have documented CH_4 leaks across urban areas tied to industrial activities, natural gas infrastructure, and landfills (e.g. (Hopkins et al., 2016; Jackson et al., 2014; Lamb et al., 2016; McKain et al., 2015). In the SLV, the averaged CH_4 mole fractions from available transects were characterized by distinct plumes, in contrast to the broad pattern of CO_2 (Fig. 6). A number of the CH_4 plumes are adjacent to industrial sources including natural gas fired power plants and a brick factory that utilizes a natural gas turbine to fire its furnace, as well as landfills.

An analysis of CH_4 during different hours of the day demonstrates the ability of a public transit platform to identify intermittent emission sources (Fig. 6b). While the CH_4 plume near the brick factory (marked by an 'K' in Fig. 6b) and natural gas fired power plant ('P' in Fig. 6b) along the Red line are present throughout the day, there is one plume ('X' in Fig. 6b) that was only present during daytime working hours, indicating a source of methane likely related to commercial or manufacturing activity. Mobile measurement campaigns that only make a few passes by any particular source (e.g. using a vehicle (Hopkins et al., 2016)) or that only operate during certain times of day or on specific days (e.g. (Apte et al., 2017) could miss intermittent sources such as those that are only present during specific times of the day or those with

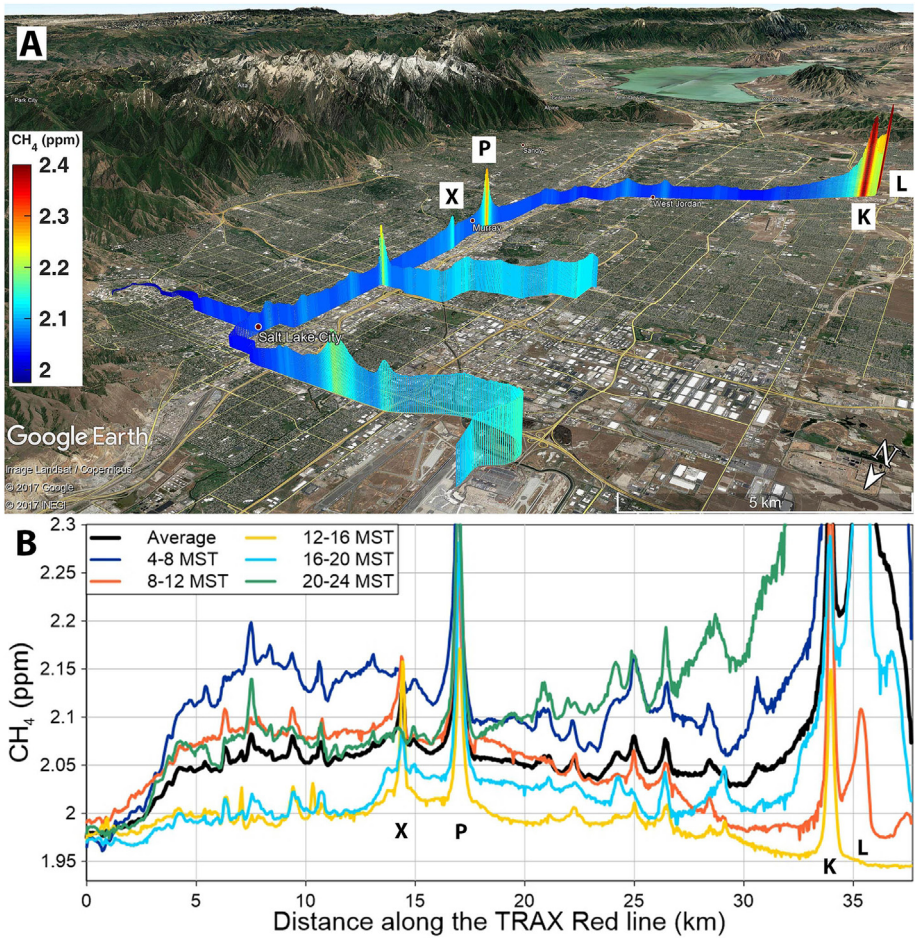

Fig. 6. Spatially and temporally averaged methane (CH_4) in the SLV between December 2014 and April 2017 (A) and average concentrations during 4-h time windows along the Red line (B). The overall average (black line) in B is the same as the Red train line data shown in A. The letters in both panels indicate the locations of an intermittent plume from an unknown source (X), a natural gas power plant (P), a brick factory that uses a natural gas fired kiln (K), and a landfill (L). (For interpretation of the references to colour in this figure legend, the reader is referred to the Web version of this article.)

episodic day-to-day variability.

3.2. Air pollutants

3.2.1. Fine particulate matter ($PM_{2.5}$)

Events when $PM_{2.5}$ concentrations exceed NAAQS in the SLV are highly episodic, so more insight can be gained by looking at specific case studies than by examining average conditions over time until numerous episodes are available to derive a climatology of various episodes (the three-year record is insufficient at this point). In January-February 2016 a study was conducted that examined how meteorological and chemical processes affected wintertime $PM_{2.5}$ during persistent cold air pools (PCAPs) (Baasandorj et al., 2017), and the TRAX observations provide additional insight into the spatial variability during this study. Fig. 7 shows several 4-hr $PM_{2.5}$ averages along the Red line during the 7–15 February 2016 pollution episode, which contained eight consecutive daily NAAQS exceedances of $PM_{2.5}$. Near the beginning of this episode on 8 February 2016 a pronounced north-south gradient in $PM_{2.5}$ was observed along the Red line (Fig. 7a). Meteorological observations from MesoWest stations ((Horel et al., 2002); Fig. 1), laser ceilometers, and lidar data from field campaigns (Baasandorj et al., 2017) as well as stationary air quality sites were utilized determine the cause of this gradient in $PM_{2.5}$ and indicated that it resulted from two factors. First, relatively clean and cool drainage flow through the gap in the southern mountain foothills and downslope katabatic flows with wind speeds between 3 and 8 m s^{-1} was observed at the southern end of the SLV that diluted the pollutants in those locales (indicated qualitatively with arrows in Fig. 7a). Second, a weak northerly flow in the northern Salt Lake Valley resulting from a lake breeze circulation resulted in a stagnation zone (Crosman and Horel, 2016) over the northern and central SLV, allowing the $PM_{2.5}$ concentrations to remain elevated there. A small but distinct plume of ~20 μg m^{-3} was observed in the south-central SLV adjacent to a gravel pit, indicated with a 'G' in Fig. 7a. A week later, on the afternoon of 14 February 2016, near the end of the pollution episode, the spatial gradient in $PM_{2.5}$ had reversed, with $PM_{2.5}$ concentrations between 20 and 30 μg m^{-3} higher over the southern portions of the SLV (Fig. 7b). In this case a partial 'mix-out' episode (Lareau and Horel, 2014) had partially removed the cold air and pollution in the Salt Lake Valley, but not in the Utah Valley. The stronger cold-air pool associated with colder temperatures over the Utah Valley to the south resulted in a density-driven flow of cold, polluted air that advected north into the SLV. Finally, in the evening of 14 February, top-down erosion of the PCAP (Lareau and Horel, 2014) led to a rapid decrease in $PM_{2.5}$ on the SLV benches on the north and southern ends of the TRAX Red line and left a shallow remnant polluted layer in the lowest ~150 m of the SLV (Fig. 7c). Similar meteorological and pollution patterns were observed as part of an intensive field campaign during a PCAP in February 2017 (Utah DEQ, 2018).

Patterns visible in the TRAX data at other times (but not plotted here) include clean air drainage out of the surrounding canyons into the SLV and lake breezes that can transport either clean or polluted air into

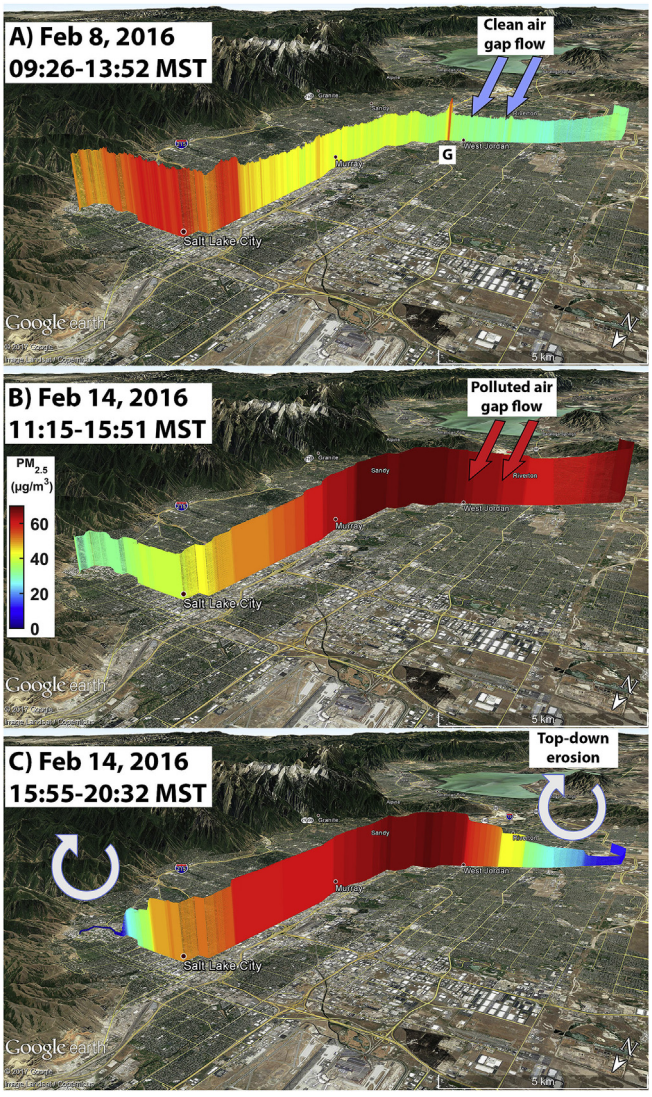

Fig. 7. Case study of the $PM_{2.5}$ evolution during a typical cold pool event in the SLV. Panels A–C show the spatial pattern of $PM_{2.5}$ during 4-h time slices. The 'G' in panel A indicates the location of a gravel pit that may have contributed to the isolated plume of $PM_{2.5}$.

the city, depending on the composition of the air over the Great Salt Lake.

In the summer, average TRAX $PM_{2.5}$ concentrations were well below the NAAQS of 35 $\mu g\, m^{-3}$ (Fig. 8). However studies have shown that adverse health effects can arise from even low pollutant concentrations (Brunekreef and Holgate, 2002; Di et al., 2017; Franklin et al., 2006) and near-road exposure to pollutants (Chen et al., 2017; Oakes et al., 2016). The TRAX average summer observations reveal numerous plumes of $PM_{2.5}$ associated with some roadways and several point sources (e.g. a gravel pit, brick factory, and an unidentified source, indicated by a 'G', 'K', and 'X' in Fig. 8).

While fine scale location-specific air quality forecasts will remain difficult to provide to the public, the observations from TRAX, in combination with a sparse network of fixed-site research and regulatory instruments and citizen-science network of lower-cost sensors (Kelly et al., 2017), along with instruments deployed on a news helicopter (Crosman et al., 2017), provide DAQ forecasters with improved understanding of the complex intra-urban meteorological and topographical factors that control pollutant concentrations.

3.2.2. Ozone (O_3)

Periods of high summertime O_3 are typically enhanced by stagnant high pressure and high temperature; however, there are also occasional episodic periods of high O_3 resulting from smoke from wildfires and lake breezes (Horel et al., 2016). The spatial patterns from summer-to-summer are similar, so we focus on the summer of 2015 that was investigated as part of the Great Salt Lake Summer Ozone Study (Blaylock et al., 2016; Horel et al., 2016). The average O_3 concentrations from available TRAX transects in the summer of 2015 were 5–10 ppb lower in the urban corridor compared to the foothills (Fig. 9a). This pattern, however, changed throughout the day with midday concentrations being homogeneous across the city while the depletion in the urban corridor occurred entirely in the evening and morning hours when residual O_3 was preferentially destroyed by enhanced nocturnal NO_x build-up in the urban corridor (Fig. 9b). These distinct spatial patterns could allow for the comparison with spatial patterns in health impacts from O_3 that may lead to advances in understanding of O_3-related health risks. In addition to the broad spatial patterns, areas of high-density traffic routes that are sources of NO_x emissions from vehicles had sharp reductions in O_3 from near-field chemical destruction of O_3 that occurred throughout the day. These areas of depleted O_3 were evident along the freeways and are discussed in greater detail in the following sections.

3.2.3. Nitrogen dioxide (NO_2)

The average distribution of NO_2 across the SLV showed similar spatial patterns as CO_2 ($r = 0.83$) and a strong anti-correlation with O_3 (Fig. 10). The broad pattern shows NO_2 concentrations that were highest in the urban core and lowest along the urban periphery. Localized enhancements were visible along many of the roadways. These spatial patterns can be more clearly understood in relation to the other species that we measured, and a discussion of these relationships follows.

3.3. O_3-NO_2-CO_2 relationships

Additional insight and an improved understanding of the factors controlling urban air composition can be gained by examining the relationships between several species (Fig. 11). First, we discuss how O_3 and NO_2 are related through atmospheric chemistry; second, we examine the relationship between NO_2 and CO_2, which are related through the combustion of fossil fuels.

The O_3-NO_2 chemistry is well known (U.S. EPA, 2013), and the strong anti-correlation between O_3 and NO_2 ($r = -0.96$) was a result of titration of O_3 by reaction with NO to form NO_2 ($NO + O_3 \rightarrow NO_2$). This is particularly evident by examining the shaded regions of Fig. 11 where the train cars were in the middle of traffic in the downtown region (A), and crossed I-15, the major north-south interstate route in the SLV (B, C, and D). These instances reflect the atmospheric chemistry near highly-traveled roadways, but similar smaller features were observed near smaller roadways as well. These results, obtained with a single set of instruments, are similar to what would be expected from a large field campaign examining distance to road relationships, illustrating the utility of public transit platforms for urban air quality studies. Future work should add nitric oxide (NO) to the measurement suite to determine NO_x ($\equiv NO + NO_2$) and these observations could be used to improve our ability to model pollutants across the city and thereby improve high-resolution pollution exposure assessments. Understanding these processes will be important as energy efficiency and adoption of electric vehicles alter emissions patterns in urban centers. Prior modeling work has shown that future urban NO_x emission reductions will lead to changes in the temporal patterns of urban O_3, resulting in higher nighttime O_3 and lower daytime O_3 (Pfister et al., 2014), and the TRAX platform is well suited to observe these changes across an entire urban center in real time.

To explore the relationship between NO_2 and CO_2, we calculated the

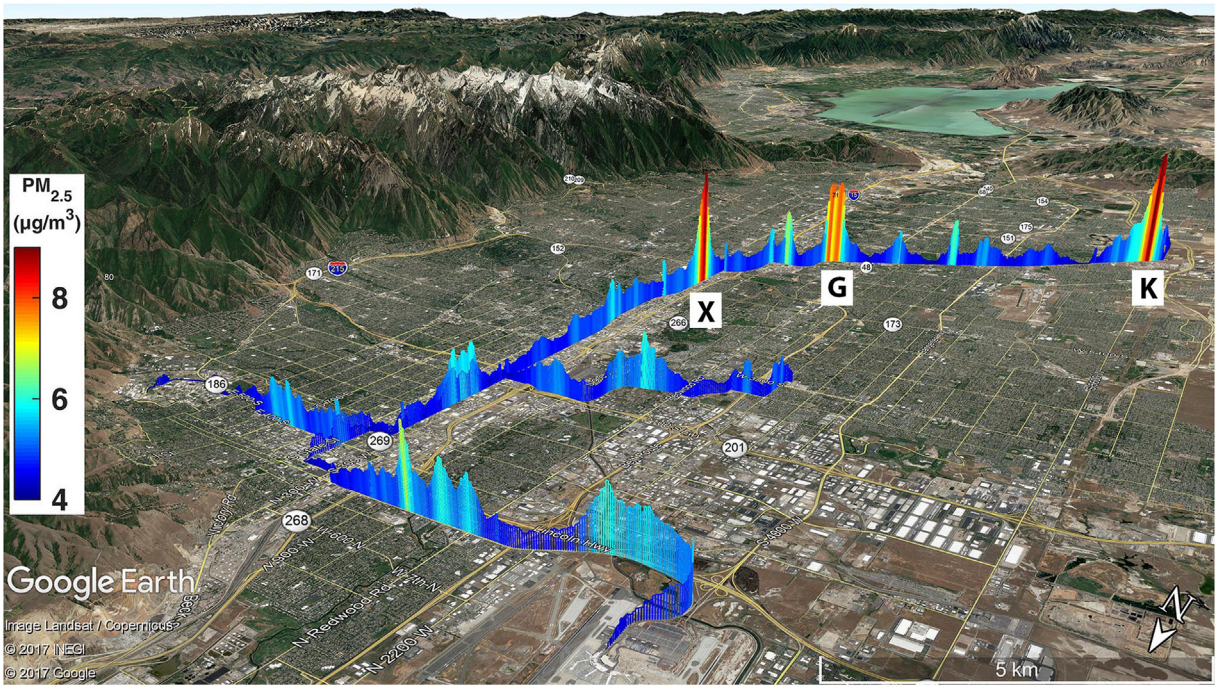

Fig. 8. $PM_{2.5}$ averaged over the summer of 2016 (May through September). The 'G', 'K', and 'X' indicate the locations of the gravel pit shown in Fig. 7a, the brick factory shown in Fig. 5 and 6, and an unidentified $PM_{2.5}$ source, respectively.

excess NO_2 and CO_2 concentrations by subtracting a qualitative estimate of background conditions (4 ppb NO_2 and 405 ppm CO_2, slightly below the minimum in the spatial averages in Fig. 11) and then calculating the excess NO_2/CO_2 (ppb/ppm) ratio. Both NO (which is quickly titrated to NO_2 by O_3) and CO_2 are co-emitted during the combustion of fossil fuels, but the ratio between them differs by source sector, fuel type, as well as vehicle speed, weight, age, and other factors (Jung et al., 2011). The impact of these differences can be most clearly seen by comparing the fine scale variations in the ratio in the shaded regions A-C in Fig. 11. In region A the train was in the middle of traffic on surface streets in downtown and the ratio was low. In contrast, in regions B and C where the train crossed the I-15 interstate with a different vehicle fleet composition moving at faster speeds, there were small peaks in the ratio. These observations provide useful targets for future work evaluating vehicle emissions in real world driving conditions and can also be compared to ratios measured at stationary tower sites during episodic periods of poor air quality (Bares et al., 2018).

Fig. 12 shows an expanded view of the shaded region D from Fig. 11 where a large persistently elevated NO_2 plume was seen. A close examination reveals that the NO_2 plume had two sub-peaks. The NO_2 peak at ~16.4 km where the Green line crossed I-15 was coincident with a narrow peak in CO_2, and because there was a proportional increase in both species at this location there was a negligible effect on the excess NO_2/CO_2 ratio (red shading). Conversely, the peak centered at ~16.8 km (blue line) is more clearly resolved in the excess NO_2/CO_2 ratio that reveals a much larger and broader NO_2 plume and suggests that the NO_x emissions from the freeway traffic were small compared to this other source. This second peak was centered over a Union Pacific rail yard 0.4 km west of the I-15 freeway that uses diesel powered switchyard locomotives to move rail cars around the rail yard (the location of the rail yard can be more clearly seen in the Google Earth KMZ supplementary materials). These switchyard locomotives comply with older (Tier 0 or 0+) locomotive emission standards (Sowards, G., personal communication, 2017) that have a high NO_x/CO_2 emission ratio (U.S. EPA, 2016). The north-south extent of the excess NO_2/CO_2 ratio can be observed along the Red line for ~6 km (between ~8 and 14 km, Fig. 11). Since these values were averaged over an extended time period, it is expected that day-to-day wind conditions would spread this plume of higher NO_2 in different directions across the SLV. Upgrading the switchyard locomotives to newer models (Tier 4) would reduce NO_x emissions by 90% and may be a cost-effective way to reduce emissions of this air pollutant (U.S. EPA, 2016).

These relationships illustrate the variety of impacts that fossil fuel combustion has on the composition of urban air. By measuring both GHGs and air pollutants, it will be possible to gain a greater understanding of the complex relationships between these species during different seasons and times of day as a result of emissions from anthropogenic and natural (e.g. biogenic) sources as well as secondary atmospheric chemical reactions. As efforts to improve air quality or reduce GHG emissions lead to lower emissions in urban centers, measurement platforms that have the ability to monitor these species across space and time will be able to track the evolution of urban air composition across cities in a unique way.

3.4. Future directions

We continue to collect data in real-time from the TRAX platforms. The long-term data archive, combined with other research and regulatory air quality observational networks, provide the opportunity to establish the Salt Lake Valley as an interdisciplinary laboratory for continued health science and air quality research that would benefit the public, urban planners, policy makers, and air quality forecasters. The research-grade instrumentation installed on the light rail train also has potential future value as a tethering system for calibrating lower-cost air quality sensors spatially distributed along the rail line. Utilizing public transit for urban atmospheric monitoring also provides a proof of concept that could be implemented in other urban regions throughout the world.

Disseminating real-time public transit air quality observations can be a powerful tool for science communication and could potentially boost public transit ridership. By taking public transit, customers can contribute to air quality monitoring while also reducing their own emissions and therefore improving air quality. Since ridership depends on factors such as satisfaction, perceived value, and personal

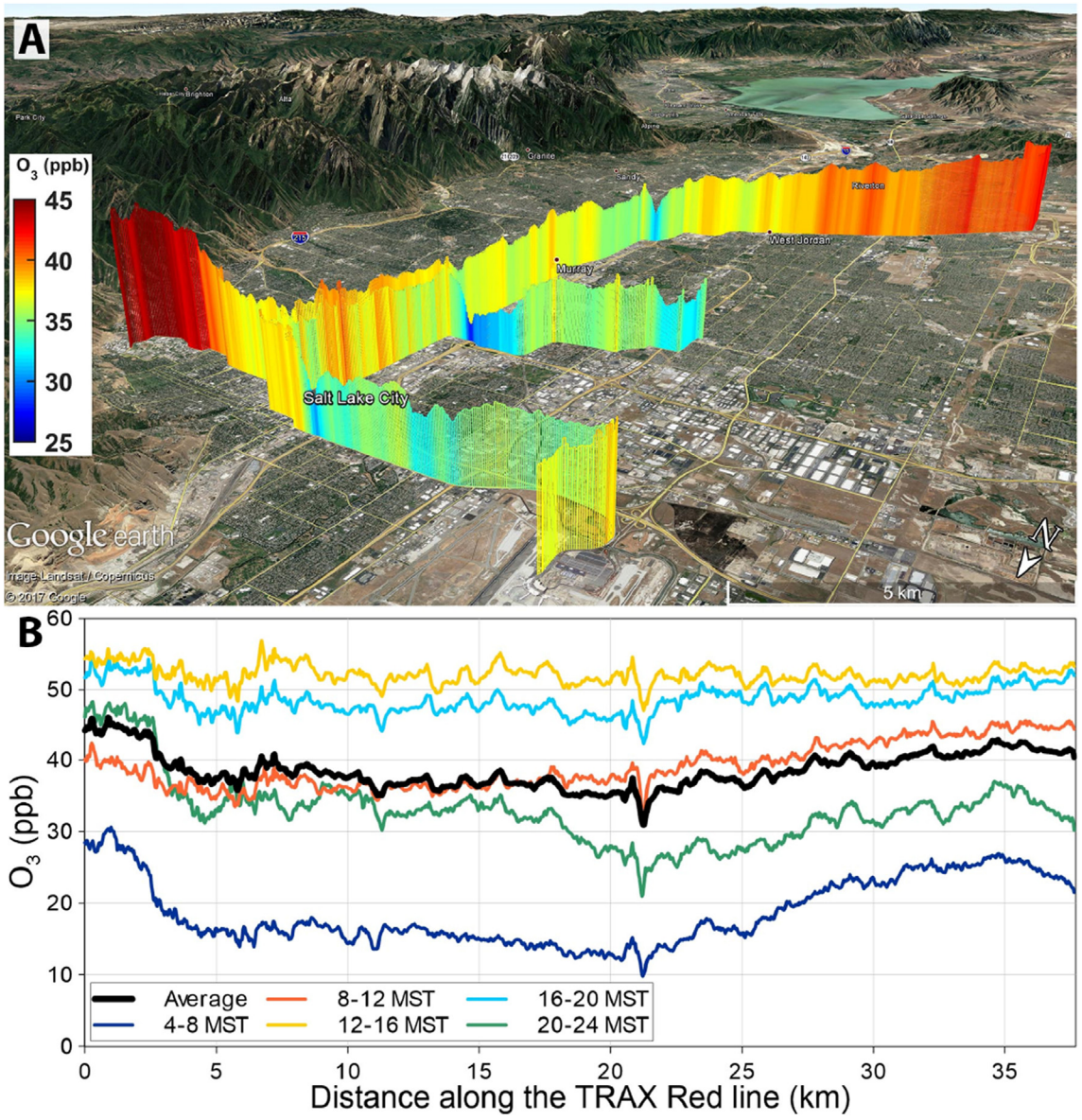

Fig. 9. The ozone (O_3) average during the summer season from May to September 2015 in the SLV (A) and average concentrations during 4-h time windows along the Red train line (B). The overall average (black line) in B is the same as the Red line data shown in A. (For interpretation of the references to colour in this figure legend, the reader is referred to the Web version of this article.)

involvement (Lai and Chen, 2011), the partnership established here with the public transit authority could increase the perceived value of public transit and increase ridership.

The repetitive nature of the TRAX transects gives insight into many processes that control the urban atmosphere and its linkages with human health and socioeconomic activities. The spatial extent of the TRAX rail network provides an excellent framework for these data to be used in combination with fixed observations sites to evaluate urban emission modeling and emission inventories of multiple species. Measurements of CO_2 could be used to monitor urban fossil fuel emissions and evaluate progress towards emission reduction targets such as Salt Lake City's goal of reducing greenhouse gas emissions by 50% in 2030 and 80% by 2040 compared to a baseline in 2009 (Salt Lake City Corporation, 2016). For CH_4, examining and modeling the temporal signature of emissions from point sources could lead to new insight into the processes causing fugitive emissions (i.e. if they are associated with leaking infrastructure or if they are associated with operations). Integrating air quality observations from available sources could be used to improve atmospheric models and estimates of pollutant exposure across urban areas and investigate the relationship with demographic characteristics and environmental justice issues. These observations and models could then be tied to spatially explicit human health impacts to improve our understanding of dose-response relationships at fine spatial scales across urban areas, which is relevant for public stakeholders and policymakers. These observations could also be used within a multi-species framework that leverages different emission patterns to reduce uncertainties in atmospheric transport, particularly during persistent cold air pools that are challenging to model and result in frequent violation of NAAQS. Also, the spatial footprint of the TRAX network (~25 km North-South and ~15 km East-West) may be suitable for ground-based evaluation of remote sensing instruments (i.e. satellite and aircraft) that are increasing their resolution to understand urban emissions and other processes with fine spatial variability. These data could also be used to compare and evaluate and calibrate high-density networks of low-cost instruments, such as the Purple Air network of low-cost air quality sensors (Kelly et al., 2017). Improving our understanding of urban GHG emissions and air pollutants will give policy makers vital information that will enable

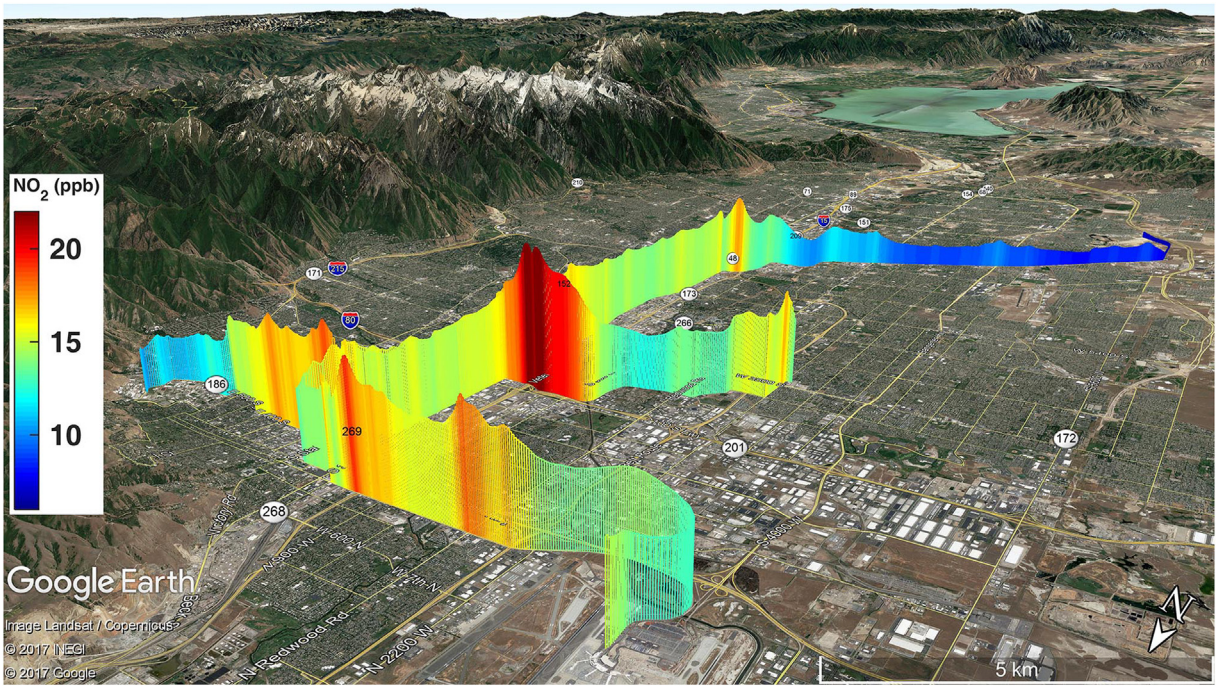

Fig. 10. The nitrogen dioxide (NO_2) average over one year from June 2016 to June 2017.

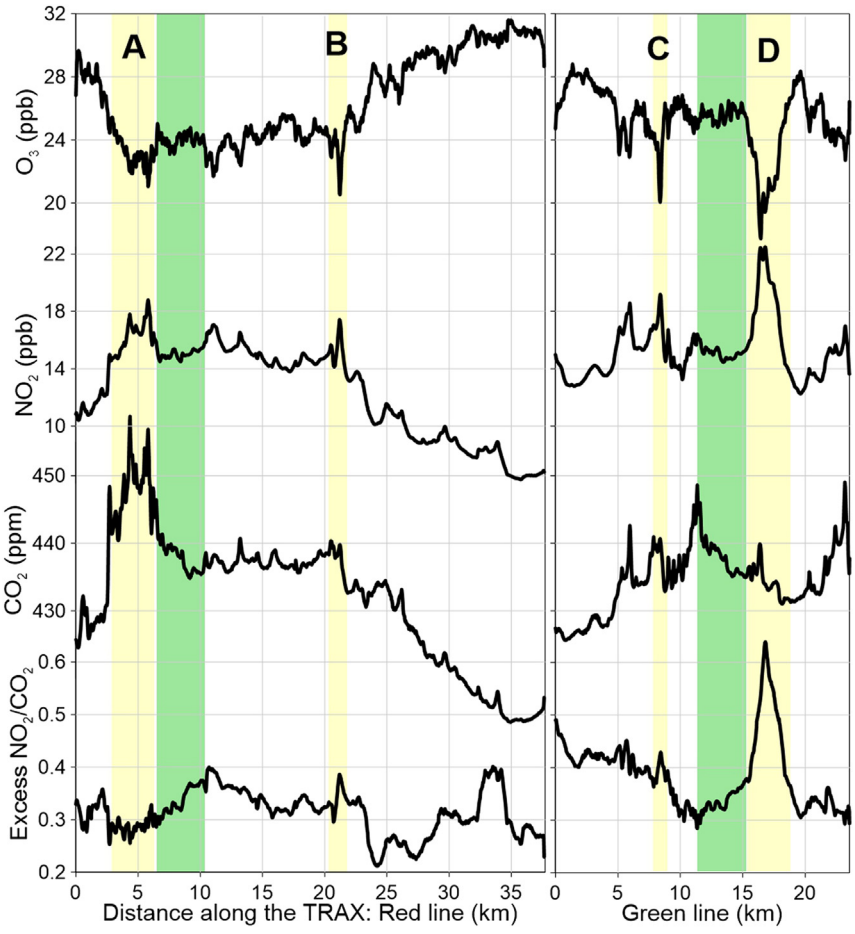

Fig. 11. Temporally averaged O_3, NO_2, CO_2 and the excess NO_2/CO_2 ratio along both of the TRAX lines. O_3 and NO_2 were measured on TRAX 2 while CO_2 was measured on TRAX 1, however since they consist of > 1 year of data, the averages can be compared to each other. The yellow shaded areas indicate where the TRAX line is in the middle of a roadway near downtown (A), and crosses I-15 on the Red line (B) and on the Green line (C and D). The green shading indicates where the Red and Green train lines overlap each other. (For interpretation of the references to colour in this figure legend, the reader is referred to the Web version of this article.)

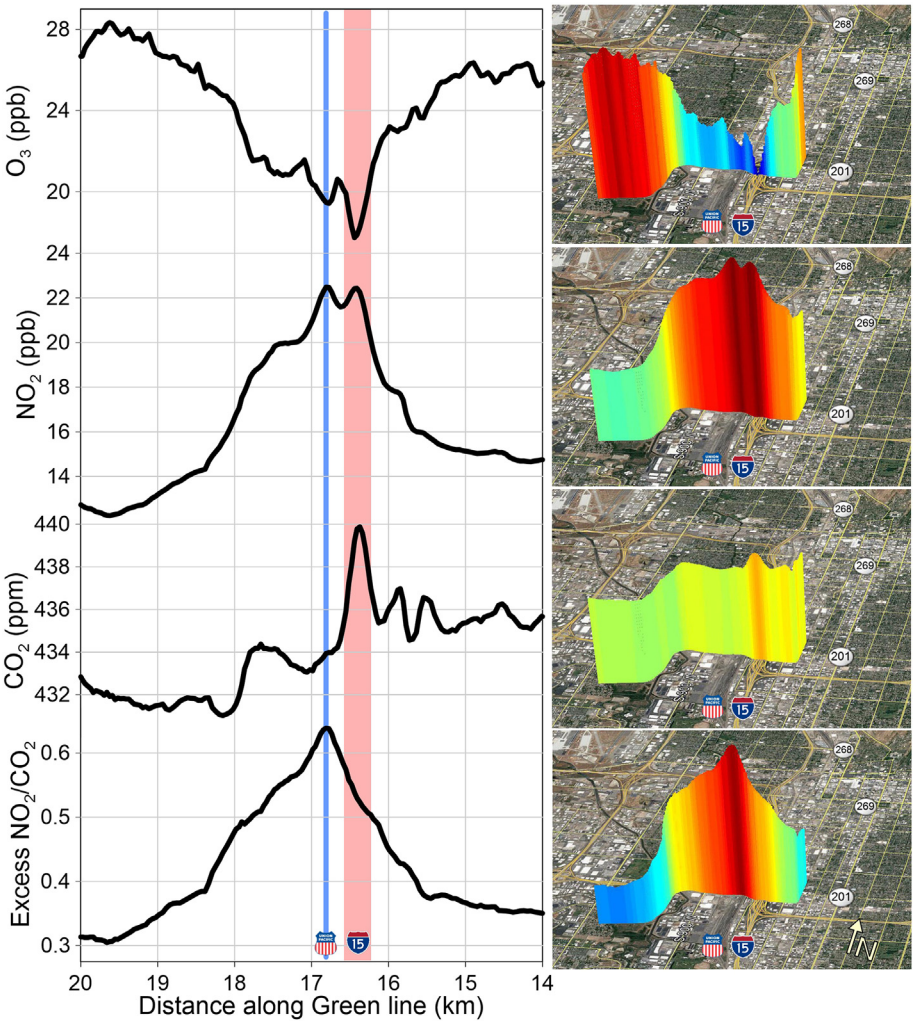

Fig. 12. Relationships between species illustrating sources of NO_2 and CO_2 along a subsection of the Green line. The Union Pacific rail yard and I-15 interstate highway are indicated with a blue line and red shading respectively in the left panel and with icons in both the left and right panels. The scale in the left panels corresponds to the shading in the right panels. Note that these Google Earth images are looking northwest to see the Union Pacific rail yard that is just south of the TRAX rail line, whereas the prior Google Earth images were looking southeast. (For interpretation of the references to colour in this figure legend, the reader is referred to the Web version of this article.)

them to plan for how future urban growth will affect emissions and air quality. Finally, the real-time data can be used directly by the public to make informed decisions about their personal exposure to pollutants during their daily activities (e.g. recreation), and social scientists could study how access to spatially explicit real-time air quality information affects behavior.

While this initial study utilized only two light-rail train cars, it demonstrates the potential for leveraging public transit vehicles as a monitoring platform. This measurement strategy provides a cost-effective way to obtain spatial and temporal coverage across urban areas where GHG emissions and air quality health impacts are concentrated. Other modes of public transit (e.g. electric buses) could also be developed to expand this measurement strategy to other cities to better understand air quality across urban areas worldwide.

Acknowledgements

The authors are grateful to the Utah Transit Authority (UTA) for supporting the installation of air quality sensors on their light rail trains. Special thanks go to James (Tal) Brooks, Teresa Jessen, Dan Christenson, William Patterson, and Elijah Jackson at UTA for assistance with the equipment installation and ongoing access to the trains for maintenance. We also thank the Center for High Performance Computing at the University of Utah for their support and resources, Google Earth for data visualization, Maria Garcia for calibration tanks, Ryan Bares and the DAQ for providing stationary site measurements for comparisons, LGR for loaning us their NO_2 analyzer, Munkhbayar Baasandorj, the DAQ, and the NOAA ESRL Twin Otter aircraft group for assistance with calibration of the NO_2 analyzer, and two anonymous reviewers who provided constructive feedback that improved the manuscript. This work was partially supported by grants from the Utah DAQ (150697), NSF (EF-1137336, OAC-1443046), NOAA (NA14OAR4310178) and DOE (DE-SC0010625).

Appendix A. Supplementary data

Supplementary data related to this article can be found at http://dx.doi.org/10.1016/j.atmosenv.2018.05.044.

Declarations of interest

None.

References

Air Quality Research Subcommittee, 2013. Air Quality Observation Systems in the United States. Committee on Environment, Natural Resources, and Sustainability.

Apte, J.S., Messier, K.P., Gani, S., Brauer, M., Kirchstetter, T.W., Lunden, M.M., Marshall, J.D., Portier, C.J., Vermeulen, R.C.H., Hamburg, S.P., 2017. High-resolution air pollution mapping with Google street view cars: exploiting big data. Environ. Sci. Technol. 51, 6999–7008. https://doi.org/10.1021/acs.est.7b00891.

Baasandorj, M., Hoch, S.W., Bares, R., Lin, J.C., Brown, S.S., Millet, D.B., Martin, R., Kelly, K., Zarzana, K.J., Whiteman, C.D., Dube, W.P., Tonnesen, G., Jaramillo, I.C., Sohl, J., 2017. Coupling between chemical and meteorological processes under persistent cold-air pool conditions: evolution of wintertime PM2.5 pollution events and N2O5 observations in Utah's Salt Lake valley. Environ. Sci. Technol. 51, 5941–5950. https://doi.org/10.1021/acs.est.6b06603.

Baldauf, R., Thoma, E., Hays, M., Shores, R., Kinsey, J., Gullett, B., Kimbrough, S., Isakov, V., Long, T., Snow, R., Khlystov, A., Weinstein, J., Chen, F.-L., Seila, R., Olson, D., Gilmour, I., Cho, S.-H., Watkins, N., Rowley, P., Bang, J., 2008. Traffic and meteorological impacts on near-road air quality: summary of methods and trends from the raleigh near-road study. J. Air Waste Manag. Assoc. 58, 865–878. https://doi.org/10.3155/1047-3289.58.7.865.

Barakeh, Z.A., Breuil, P., Redon, N., Pijolat, C., Locoge, N., Viricelle, J.-P., 2017. Development of a normalized multi-sensors system for low cost on-line atmospheric pollution detection. Sensor. Actuator. B Chem. 241, 1235–1243. https://doi.org/10.1016/j.snb.2016.10.006.

Bares, R., Lin John, C., Hoch Sebastian, W., Munkhbayar, Baasandorj, Mendoza Daniel, L., Ben, Fasoli, Logan, Mitchell, Catharine Douglas, Stephens Britton B., 2018. The wintertime covariation of CO2 and criteria pollutants in an urban valley of the western United States. J. Geophys. Res. Atmospheres 0. https://doi.org/10.1002/2017JD027917.

Bateman, M., Collard, C., Teigen, S., 2016. Part I: Survey of Voters' Issues and Concerns (No. 739), 2016 Utah Priorities Project. Utah Foundation.

Blaylock, B., Horel, J.D., Crosman, E.T., 2016. Impact of lake breezes on summer ozone concentrations in the Salt Lake valley. J. Appl. Meteorol. Climatol 56, 353–370. https://doi.org/10.1175/JAMC-D-16-0216.1.

Borrego, C., Costa, A.M., Ginja, J., Amorim, M., Coutinho, M., Karatzas, K., Sioumis, T., Katsifarakis, N., Konstantinidis, K., De Vito, S., Esposito, E., Smith, P., André, N., Gérard, P., Francis, L.A., Castell, N., Schneider, P., Viana, M., Minguillón, M.C., Reimringer, W., Otjes, R.P., von Sicard, O., Pohle, R., Elen, B., Suriano, D., Pfister, V., Prato, M., Dipinto, S., Penza, M., 2016. Assessment of air quality microsensors versus reference methods: the EuNetAir joint exercise. Atmos. Environ. Times 147, 246–263. https://doi.org/10.1016/j.atmosenv.2016.09.050.

Brent, L.C., Thorn, W.J., Gupta, M., Leen, B., Stehr, J.W., He, H., Arkinson, H.L., Weinheimer, A., Garland, C., Pusede, S.E., Wooldridge, P.J., Cohen, R.C., Dickerson, R.R., 2013. Evaluation of the use of a commercially available cavity ringdown absorption spectrometer for measuring NO2 in flight, and observations over the Mid-Atlantic States, during DISCOVER-AQ. J. Atmos. Chem. 72, 503–521. https://doi.org/10.1007/s10874-013-9265-6.

Brunekreef, B., Holgate, S.T., 2002. Air pollution and health. Lancet 360, 1233–1242. https://doi.org/10.1016/S0140-6736(02)11274-8.

Castell, N., Kobernus, M., Liu, H.-Y., Schneider, P., Lahoz, W., Berre, A.J., Noll, J., 2015. Mobile technologies and services for environmental monitoring: the Citi-Sense-MOB approach. Urban Clim. New Sensing Technologies and Methods for Air Pollution Monitoring 14 (Part 3), 370–382. https://doi.org/10.1016/j.uclim.2014.08.002.

Castellini, S., Moroni, B., Cappelletti, D., 2014. PMetro: measurement of urban aerosols on a mobile platform. Measurement 49, 99–106. https://doi.org/10.1016/j.measurement.2013.11.045.

Chen, H., Kwong, J.C., Copes, R., Tu, K., Villeneuve, P.J., Donkelaar, A., van, Hystad, P., Martin, R.V., Murray, B.J., Jessiman, B., Wilton, A.S., Kopp, A., Burnett, R.T., 2017. Living near major roads and the incidence of dementia, Parkinson's disease, and multiple sclerosis: a population-based cohort study. Lancet 389, 718–726. https://doi.org/10.1016/S0140-6736(16)32399-6.

Christen, A., Coops, N.C., Crawford, B.R., Kellett, R., Liss, K.N., Olchovski, I., Tooke, T.R., van der Laan, M., Voogt, J.A., 2011. Validation of modeled carbon-dioxide emissions from an urban neighborhood with direct eddy-covariance measurements. Atmos. Environ. 45, 6057–6069. https://doi.org/10.1016/j.atmosenv.2011.07.040.

Clements, A.L., Griswold, W.G., Rs, A., Johnston, J.E., Herting, M.M., Thorson, J., Collier-Oxandale, A., Hannigan, M., 2017. Low-cost air quality monitoring tools: from research to practice (a workshop summary). Sensors 17 (2478). https://doi.org/10.3390/s17112478.

Correia, A.W., Pope, C.A., Dockery, D.W., Wang, Y., Ezzati, M., Dominici, F., 2013. The effect of air pollution control on life expectancy in the United States: an analysis of 545 us counties for the period 2000 to 2007. Epidemiol. Camb. Mass 24, 23–31. https://doi.org/10.1097/EDE.0b013e3182770237.

Crosman, E.T., Horel, J.D., 2016. Winter lake breezes near the Great Salt Lake. Bound.-Layer Meteorol 159, 439–464. https://doi.org/10.1007/s10546-015-0117-6.

Crosman, E.T., Jacques, A.A., Horel, J.D., 2017. A novel approach for monitoring vertical profiles of boundary-layer pollutants: utilizing routine news helicopter flights. Atmospheric Pollut. Res. 8, 828–835. https://doi.org/10.1016/j.apr.2017.01.013.

Deville Cavellin, L., Weichenthal, S., Tack, R., Ragettli, M.S., Smargiassi, A., Hatzopoulou, M., 2016. Investigating the use of portable air pollution sensors to capture the spatial variability of traffic-related air pollution. Environ. Sci. Technol. 50, 313–320. https://doi.org/10.1021/acs.est.5b04235.

Di, Q., Wang, Yan, Zanobetti, A., Wang, Yun, Koutrakis, P., Choirat, C., Dominici, F., Schwartz, J.D., 2017. Air pollution and mortality in the medicare population. N. Engl. J. Med. 376, 2513–2522. https://doi.org/10.1056/NEJMoa1702747.

Dlugokencky, E.J., Myers, R.C., Lang, P.M., Masarie, K.A., Crotwell, A.M., Thoning, K.W., Hall, B.D., Elkins, J.W., Steele, L.P., 2005. Conversion of NOAA atmospheric dry air CH4 mole fractions to a gravimetrically prepared standard scale. J. Geophys. Res.-Atmospheres 110, 8.

Franklin, M., Zeka, A., Schwartz, J., 2006. Association between PM2.5 and all-cause and specific-cause mortality in 27 US communities. J. Expo. Sci. Environ. Epidemiol. 17, 279–287. https://doi.org/10.1038/sj.jes.7500530.

Gozzi, F., Della Ventura, G., Marcelli, A., 2016. Mobile monitoring of particulate matter: state of art and perspectives. Atmospheric Pollut. Res. 7, 228–234. https://doi.org/10.1016/j.apr.2015.09.007.

Gurney, K.R., Mendoza, D.L., Zhou, Y., Fischer, M.L., Miller, C.C., Geethakumar, S., de la Rue du Can, S., 2009. High resolution fossil fuel combustion CO2 emission fluxes for the United States. Environ. Sci. Technol. 43, 5535–5541. https://doi.org/10.1021/es900806c.

Gurney, K.R., Romero-Lankao, P., Seto, K.C., Hutyra, L.R., Duren, R., Kennedy, C., Grimm, N.B., Ehleringer, J.R., Marcotullio, P., Hughes, S., Pincetl, S., Chester, M.V., Runfola, D.M., Feddema, J.J., Sperling, J., 2015. Climate change: track urban emissions on a human scale. Nature 525, 179–181. https://doi.org/10.1038/525179a.

Hagemann, R., Corsmeier, U., Kottmeier, C., Rinke, R., Wieser, A., Vogel, B., 2014. Spatial variability of particle number concentrations and NOx in the Karlsruhe (Germany) area obtained with the mobile laboratory 'AERO-TRAM.'. Atmos. Environ. 94, 341–352. https://doi.org/10.1016/j.atmosenv.2014.05.051.

Hasenfratz, D., Saukh, O., Walser, C., Hueglin, C., Fierz, M., Arn, T., Beutel, J., Thiele, L., 2015. Deriving high-resolution urban air pollution maps using mobile sensor nodes. Pervasive Mob. Comput.. In: Selected Papers from the Twelfth Annual IEEE International Conference on Pervasive Computing and Communications (PerCom 2014), vol. 16. pp. 268–285. Part B. https://doi.org/10.1016/j.pmcj.2014.11.008.

Hoek, G., Beelen, R., de Hoogh, K., Vienneau, D., Gulliver, J., Fischer, P., Briggs, D., 2008. A review of land-use regression models to assess spatial variation of outdoor air pollution. Atmos. Environ. 42, 7561–7578. https://doi.org/10.1016/j.atmosenv.2008.05.057.

Hopkins, F.M., Kort, E.A., Bush, S.E., Ehleringer, J.R., Lai, C.-T., Blake, D.R., Randerson, J.T., 2016. Spatial patterns and source attribution of urban methane in the Los Angeles Basin. J. Geophys. Res. Atmospheres 121 2015JD024429. https://doi.org/10.1002/2015JD024429.

Horel, J., Crosman, E., Jacques, A., Blaylock, B., Arens, S., Long, A., Sohl, J., Martin, R., 2016. Summer ozone concentrations in the vicinity of the Great Salt Lake. Atmos. Sci. Lett. 17, 480–486. https://doi.org/10.1002/asl.680.

Horel, J., Splitt, M., Dunn, L., Pechmann, J., White, B., Ciliberti, C., Lazarus, S., Slemmer, J., Zaff, D., Burks, J., 2002. Mesowest: cooperative mesonets in the western United States. Bull. Am. Meteorol. Soc. 83, 211–225.

Hutyra, L.R., Duren, R., Gurney, K.R., Grimm, N., Kort, E.A., Larson, E., Shrestha, G., 2014. Urbanization and the carbon cycle: current capabilities and research outlook from the natural sciences perspective. Earths Future 2, 473–495. https://doi.org/10.1002/2014EF000255.

Idso, C.D., Idso, S.B., Balling Jr., R.C., 2001. An intensive two-week study of an urban CO2 dome in Phoenix, Arizona, USA. Atmos. Environ. 35, 995–1000. https://doi.org/10.1016/S1352-2310(00)00412-X.

Jackson, R.B., Down, A., Phillips, N.G., Ackley, R.C., Cook, C.W., Plata, D.L., Zhao, K., 2014. Natural gas pipeline leaks across Washington, DC. Environ. Sci. Technol. 48, 2051–2058. https://doi.org/10.1021/es404474x.

Jiao, W., Hagler, G., Williams, R., Sharpe, R., Brown, R., Garver, D., Judge, R., Caudill, M., Rickard, J., Davis, M., Weinstock, L., Zimmer-Dauphinee, S., Buckley, K., 2016. Community Air Sensor Network (CAIRSENSE) project: evaluation of low-cost sensor performance in a suburban environment in the southeastern United States. Atmos Meas Tech 9, 5281–5292. https://doi.org/10.5194/amt-9-5281-2016.

Jung, S., Lee, M., Kim, J., Lyu, Y., Park, J., 2011. Speed-dependent emission of air pollutants from gasoline-powered passenger cars. Environ. Technol. 32, 1173–1181. https://doi.org/10.1080/09593330.2010.505611.

Kelly, K.E., Whitaker, J., Petty, A., Widmer, C., Dybwad, A., Sleeth, D., Martin, R., Butterfield, A., 2017. Ambient and laboratory evaluation of a low-cost particulate matter sensor. Environ. Pollut. 221, 491–500. https://doi.org/10.1016/j.envpol.2016.12.039.

Kumar, P., Morawska, L., Martani, C., Biskos, G., Neophytou, M., Di Sabatino, S., Bell, M., Norford, L., Britter, R., 2015. The rise of low-cost sensing for managing air pollution in cities. Environ. Int. 75, 199–205. https://doi.org/10.1016/j.envint.2014.11.019.

Lai, W.-T., Chen, C.-F., 2011. Behavioral intentions of public transit passengers—the roles of service quality, perceived value, satisfaction and involvement. Transport Pol. 18, 318–325. https://doi.org/10.1016/j.tranpol.2010.09.003.

Lamb, B.K., Cambaliza, M.O.L., Davis, K.J., Edburg, S.L., Ferrara, T.W., Floerchinger, C., Heimburger, A.M.F., Herndon, S., Lauvaux, T., Lavoie, T., Lyon, D.R., Miles, N., Prasad, K.R., Richardson, S., Roscioli, J.R., Salmon, O.E., Shepson, P.B., Stirm, B.H., Whetstone, J., 2016. Direct and indirect measurements and modeling of methane emissions in indianapolis, Indiana. Environ. Sci. Technol. 50, 8910–8917. https://doi.org/10.1021/acs.est.6b01198.

Landrigan, P.J., Fuller, R., Acosta, N.J.R., Adeyi, O., Arnold, R., Basu, N.N., Baldé, A.B., Bertollini, R., Bose-O'Reilly, S., Boufford, J.I., Breysse, P.N., Chiles, T., Mahidol, C., Coll-Seck, A.M., Cropper, M.L., Fobil, J., Fuster, V., Greenstone, M., Haines, A., Hanrahan, D., Hunter, D., Khare, M., Krupnick, A., Lanphear, B., Lohani, B., Martin, K., Mathiasen, K.V., McTeer, M.A., Murray, C.J.L., Ndahimananjara, J.D., Perera, F., Potočnik, J., Preker, A.S., Ramesh, J., Rockström, J., Salinas, C., Samson, L.D., Sandilya, K., Sly, P.D., Smith, K.R., Steiner, A., Stewart, R.B., Suk, W.A., Schayck, O.C.P. van, Yadama, G.N., Yumkella, K., Zhong, M., October 19, 2017. The Lancet Commission on pollution and health. Lancet 391 (10119), 462–512. https://doi.org/10.1016/S0140-6736(17)32345-0.

Lareau, N.P., Horel, J.D., 2015. Dynamically induced displacements of a persistent cold-air pool. Bound.-Layer Meteorol 154, 291–316. https://doi.org/10.1007/s10546-014-9968-5.

Lareau, N.P., Horel, J.D., 2014. Turbulent erosion of persistent cold-air pools: numerical simulations. J. Atmos. Sci. 72, 1409–1427. https://doi.org/10.1175/JAS-D-14-0173.1.

Le Quéré, C., Andrew, R.M., Canadell, J.G., Sitch, S., Korsbakken, J.I., Peters, G.P., Manning, A.C., Boden, T.A., Tans, P.P., Houghton, R.A., Keeling, R.F., Alin, S., Andrews, O.D., Anthoni, P., Barbero, L., Bopp, L., Chevallier, F., Chini, L.P., Ciais, P., Currie, K., Delire, C., Doney, S.C., Friedlingstein, P., Gkritzalis, T., Harris, I., Hauck, J., Haverd, V., Hoppema, M., Klein Goldewijk, K., Jain, A.K., Kato, E., Körtzinger, A., Landschützer, P., Lefèvre, N., Lenton, A., Lienert, S., Lombardozzi, D., Melton, J.R., Metzl, N., Millero, F., Monteiro, P.M.S., Munro, D.R., Nabel, J.E.M.S., Nakaoka, S., O'Brien, K., Olsen, A., Omar, A.M., Ono, T., Pierrot, D., Poulter, B., Rödenbeck, C., Salisbury, J., Schuster, U., Schwinger, J., Séférian, R., Skjelvan, I., Stocker, B.D., Sutton, A.J., Takahashi, T., Tian, H., Tilbrook, B., Laan-Luijkx, I.T., van der, Werf, van

der, G.R., Viovy, N., Walker, A.P., Wiltshire, A.J., Zaehle, S., 2016. Global carbon budget 2016. Earth Syst. Sci. Data 8, 605–649. https://doi.org/10.5194/essd-8-605-2016.

Lee, J.K., Christen, A., Ketler, R., Nesic, Z., 2017. A mobile sensor network to map carbon dioxide emissions in urban environments. Atmos Meas Tech 10, 645–665. https://doi.org/10.5194/amt-10-645-2017.

Lin, J.C., Mitchell, L., Crosman, E., Mendoza, D., Buchert, M., Bares, R., Fasoli, B., Bowling, D.R., Pataki, D., Catharine, D., Strong, C., Gurney, K., Patarasuk, R., Baasandorj, M., Jacques, A., Hoch, S., Horel, J., Ehleringer, J., in press. CO_2 and carbon emissions from cities: linkages to air quality, socioeconomic activity and stakeholders in the Salt Lake City urban area. BAMS.

Mallia, D.V., Kochanski, A., Wu, D., Pennell, C., Oswald, W., Lin, J.C., 2017. Wind-blown dust modeling using a Backward-Lagrangian particle dispersion model. J. Appl. Meteorol. Climatol 56, 2845–2867. https://doi.org/10.1175/JAMC-D-16-0351.1.

Mallia, D.V., Lin, J.C., Urbanski, S., Ehleringer, J., Nehrkorn, T., 2015. Impacts of upwind wildfire emissions on CO, CO2, and PM2.5 concentrations in Salt Lake City. Utah. J. Geophys. Res. Atmospheres 120 2014JD022472. https://doi.org/10.1002/2014JD022472.

Matte, T.D., Ross, Z., Kheirbek, I., Eisl, H., Johnson, S., Gorczynski, J.E., Kass, D., Markowitz, S., Pezeshki, G., Clougherty, J.E., 2013. Monitoring intraurban spatial patterns of multiple combustion air pollutants in New York City: design and implementation. J. Expo. Sci. Environ. Epidemiol. 23, 223–231. https://doi.org/10.1038/jes.2012.126.

Mays, K.L., Shepson, P.B., Stirm, B.H., Karion, A., Sweeney, C., Gurney, K.R., 2009. Aircraft-based measurements of the carbon footprint of indianapolis. Environ. Sci. Technol. 43, 7816–7823. https://doi.org/10.1021/es901326b.

McKain, K., Down, A., Raciti, S.M., Budney, J., Hutyra, L.R., Floerchinger, C., Herndon, S.C., Nehrkorn, T., Zahniser, M.S., Jackson, R.B., Phillips, N., Wofsy, S.C., 2015. Methane emissions from natural gas infrastructure and use in the urban region of Boston. Massachusetts. Proc. Natl. Acad. Sci. 201416261. https://doi.org/10.1073/pnas.1416261112.

Miskell, G., Salmond, J., Alavi-Shoshtari, M., Bart, M., Ainslie, B., Grange, S., McKendry, I.G., Henshaw, G.S., Williams, D.E., 2016. Data verification tools for minimizing management costs of dense air-quality monitoring networks. Environ. Sci. Technol. 50, 835–846. https://doi.org/10.1021/acs.est.5b04421.

Mitchell, L.E., Lin, J.C., Bowling, D.R., Pataki, D.E., Strong, C., Schauer, A.J., Bares, R., Bush, S.E., Stephens, B.B., Mendoza, D., Mallia, D., Holland, L., Gurney, K.R., Ehleringer, J.R., 2018. Long-term urban carbon dioxide observations reveal spatial and temporal dynamics related to urban characteristics and growth. Proc. Natl. Acad. Sci. Unit. States Am. 115, 2912–2917. https://doi.org/10.1073/pnas.1702393115.

Oakes, M.M., Burke, J.M., Norris, G.A., Kovalcik, K.D., Pancras, J.P., Landis, M.S., 2016. Near-road enhancement and solubility of fine and coarse particulate matter trace elements near a major interstate in Detroit. Michigan. Atmos. Environ 145, 213–224. https://doi.org/10.1016/j.atmosenv.2016.09.034.

Park, Y.M., Kwan, M.-P., 2017. Individual exposure estimates may be erroneous when spatiotemporal variability of air pollution and human mobility are ignored. Health Place 43, 85–94. https://doi.org/10.1016/j.healthplace.2016.10.002.

Pataki, D.E., Bowling, D.R., Ehleringer, J.R., 2003. Seasonal cycle of carbon dioxide and its isotopic composition in an urban atmosphere: anthropogenic and biogenic effects. J. Geophys. Res.-Atmospheres 108, 1–8. https://doi.org/10.1029/2003jd003865.

Patarasuk, R., Gurney, K.R., O'Keeffe, D., Song, Y., Huang, J., Rao, P., Buchert, M., Lin, J.C., Mendoza, D., Ehleringer, J.R., 2016. Urban high-resolution fossil fuel CO2 emissions quantification and exploration of emission drivers for potential policy applications. Urban Ecosyst. 19, 1013–1039. https://doi.org/10.1007/s11252-016-0553-1.

Pfister, G.G., Walters, S., Lamarque, J.-F., Fast, J., Barth, M.C., Wong, J., Done, J., Holland, G., Bruyère, C.L., 2014. Projections of future summertime ozone over the U.S. J. Geophys. Res. Atmospheres 2013, JD020932. https://doi.org/10.1002/2013JD020932.

Pouliot, G., Pierce, T., Denier van der Gon, H., Schaap, M., Moran, M., Nopmongcol, U., 2012. Comparing emission inventories and model-ready emission datasets between Europe and North America for the AQMEII project. In: Atmos. Environ., AQMEII: an International Initiative for the Evaluation of Regional-scale Air Quality Models - Phase 1. vol. 53. pp. 4–14. https://doi.org/10.1016/j.atmosenv.2011.12.041.

Salt Lake City Corporation, 2016. A Joint Resolution of the Salt Lake City Council and Mayor Establishing Renewable Energy and Carbon Emissions Reduction Goals for Salt Lake City.

Shusterman, A.A., Teige, V.E., Turner, A.J., Newman, C., Kim, J., Cohen, R.C., 2016. The BErkeley atmospheric CO2 observation network: initial evaluation. Atmos. Chem. Phys. 16, 13449–13463. https://doi.org/10.5194/acp-16-13449-2016.

Snyder, E.G., Watkins, T.H., Solomon, P.A., Thoma, E.D., Williams, R.W., Hagler, G.S.W., Shelow, D., Hindin, D.A., Kilaru, V.J., Preuss, P.W., 2013. The changing paradigm of air pollution monitoring. Environ. Sci. Technol. 47, 11369–11377. https://doi.org/10.1021/es4022602.

Steenburgh, W.J., Massey, J.D., Painter, T.H., 2012. Episodic dust events of Utah's Wasatch front and adjoining region. J. Appl. Meteorol. Climatol 51, 1654–1669. https://doi.org/10.1175/JAMC-D-12-07.1.

Thompson, J.E., 2016. Crowd-sourced air quality studies: a review of the literature & portable sensors. Trends Environ. Anal. Chem. 11, 23–34. https://doi.org/10.1016/j.teac.2016.06.001.

UDOT, 2017. Annual average daily traffic (AADT) [www document]. URL. https://www.udot.utah.gov/main/f?p=100:pg:0::::V,T:,528, Accessed date: 3 February 2017.

U.S. EPA, 2016. Locomotives: Exhaust Emission Standards (No. EPA-420-b-16-024).

U.S. EPA, 2013. Integrated Science Assessment (ISA) of Ozone and Related Photochemical Oxidants (No. EPA/600/R-10/076F). (Washington, DC).

Utah DEQ, 2018. Utah winter fine particulate study (UWFPS) [www document]. URL. https://deq.utah.gov/legacy/programs/air-quality/research/projects/northern-ut-air-polution/winter-fine-particulate-aircraft-study.htm, Accessed date: 4 March 2018.

Van den Bossche, J., Peters, J., Verwaeren, J., Botteldooren, D., Theunis, J., De Baets, B., 2015. Mobile monitoring for mapping spatial variation in urban air quality: development and validation of a methodology based on an extensive dataset. Atmos. Environ. 105, 148–161. https://doi.org/10.1016/j.atmosenv.2015.01.017.

Venkatram, A., Isakov, V., Seila, R., Baldauf, R., 2009. Modeling the impacts of traffic emissions on air toxics concentrations near roadways. Atmos. Environ. 43, 3191–3199. https://doi.org/10.1016/j.atmosenv.2009.03.046.

Whiteman, C.D., Hoch, S.W., Horel, J.D., Charland, A., 2014. Relationship between particulate air pollution and meteorological variables in Utah's Salt Lake Valley. Atmos. Environ. 94, 742–753. https://doi.org/10.1016/j.atmosenv.2014.06.012.

Young, J.S., Whiteman, C.D., 2015. Laser ceilometer investigation of persistent wintertime cold-air pools in Utah's Salt Lake valley. J. Appl. Meteorol. Climatol 54, 752–765. https://doi.org/10.1175/JAMC-D-14-0115.1.

Zhao, C.L., Tans, P.P., 2006. Estimating uncertainty of the WMO mole fraction scale for carbon dioxide in air. J. Geophys. Res. Atmospheres 111, D08S09. https://doi.org/10.1029/2005JD006003.

Zimmerman, N., Presto, A.A., Kumar, S.P.N., Gu, J., Hauryliuk, A., Robinson, E.S., Robinson, A.L., Subramanian, R., 2017. Closing the gap on lower cost air quality monitoring: machine learning calibration models to improve low-cost sensor performance. Atmos Meas Tech Discuss 2017, 1–36. https://doi.org/10.5194/amt-2017-260.

Zivin, J.G., Neidell, M., 2018. Air pollution's hidden impacts. Science 359, 39–40. https://doi.org/10.1126/science.aap7711.